

WESLEY LIRA GABRIEL

**ELECTROCHEMICAL DEGRADATION OF IBUPROFEN AND NAPROXEN
USING ELECTRO-FENTON PROCESS MONITORED BY FLUORESCENCE
AND CHEMOMETRIC METHODS**

Dissertation submitted to the
Agrochemistry Graduate Program of the
Universidade Federal de Viçosa in partial
fulfillment of the requirements for the
degree of *Magister Scientiae*.

VIÇOSA
MINAS GERAIS - BRAZIL
2018

**Ficha catalográfica preparada pela Biblioteca Central da Universidade
Federal de Viçosa - Câmpus Viçosa**

T

G118e
2018 Gabriel, Wesley Lira, 1990-
Electrochemical degradation of ibuprofen and naproxen
using electro-fenton process monitored by fluorescence and
chemometric methods / Wesley Lira Gabriel. – Viçosa, MG,
2018.

xii, 53 f. : il. (algumas color.) ; 29 cm.

Texto em inglês.

Orientador: Reinaldo Francisco Teófilo.

Dissertação (mestrado) - Universidade Federal de Viçosa.

Referências bibliográficas: f. 48-53.

1. Eletroquímica. 2. Medicamentos. 3. Fluorescência -
Espectros. 4. Quimiometria. I. Universidade Federal de Viçosa.
Departamento de Química. Programa de Pós-Graduação em
Agroquímica. II. Título.


CDD 22. ed. 541.37

WESLEY LIRA GABRIEL

**ELECTROCHEMICAL DEGRADATION OF IBUPROFEN AND NAPROXEN
USING ELECTRO-FENTON PROCESS MONITORED BY FLUORESCENCE
AND CHEMOMETRIC METHODS**

Dissertation submitted to the
Agrochemistry Graduate Program of the
Universidade Federal Viçosa in partial
fulfillment of the requirements for the
degree of *Magister Scientiae*.

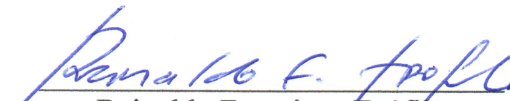
APPROVED: February 20th, 2018.



Luiz Alexandre Peternelli



Renata Pereira Lopes Moreira



Reinaldo Francisco Teófilo
(Advisor)

**In honor of
My mother Vanda, my sister Weslane, and
My grandparents Raimundo and Maria.**

**“It all works somehow in the end.”
The Strokes, Barely legal.**

ACKNOWLEDGMENTS

Agradeço a minha mãe, minha irmã e meus avós por sempre acreditarem em mim.

Ao professor Reinaldo Francisco Teófilo por aceitar me orientar e me ajudar em tudo.

Ao professor Marcos Rogério Tótola por disponibilizar o instrumento de fluorescência em seu laboratório de pesquisa.

Ao professor Antônio Augusto Neves pelo auxílio com as análises de TOC.

Ao Laboratório de Biotecnologia e Melhoramento Vegetal pela disponibilização do instrumento de HPLC.

À Universidade Federal de Viçosa que desde 2010 tem contribuído para a minha formação.

Ao Departamento de Química e ao Programa de Pós-Graduação em Agroquímica.

Aos membros da banca por aceitarem o convite.

À CAPES (Coordenação de Aperfeiçoamento de Pessoal de Nível Superior) pela bolsa concedida.

Em especial aos meus queridos amigos, Larissa, Jussara, Wilson, Ingredy, Bianca, Nathalia, Carlos, Hélder, Danilo, Paula e Ulisses por sempre escutarem minhas lamentações, me fazerem rir e estarem sempre comigo quando precisei, AMO VOCÊS SEUS LINDOS!!!

E por fim, todos aqueles que de alguma forma contribuíram para a realização deste trabalho.

SUMMARY

ABBREVIATION LIST	vii
FIGURE LIST	viii
TABLE LIST	x
ABSTRACT	xi
RESUMO.....	xii
1 INTRODUCTION.....	1
2 OBJECTIVES	3
3 LITERATURE REVIEW.....	4
3.1 Occurrence of pharmaceutical in water.....	4
3.2 Emerging Contaminants.....	5
3.3 Naproxen and Ibuprofen	6
3.4 Advanced Oxidation Processes (AOPs).....	7
3.5 Fenton process.....	8
3.6 Fluorescence spectroscopy.....	10
3.7 High-Performance Liquid Chromatography (HPLC)	11
3.8 Chemometrics	12
3.8.1 <i>Design of experiments</i>	12
3.8.2 <i>Signal resolution methods</i>	13
3.8.3 <i>Parallel factor analyses</i>	13
3.8.4 <i>Multivariate curve resolution-alternating least squares</i>	16
3.8.5 <i>Partial Least Squares Regression</i>	18
4 MATERIALS AND METHODS.....	19
4.1 Chemicals.....	19
4.2 BDD Anode.....	19
4.3 Electrochemical cell	19
4.4 Degradation system.....	20
4.5 2^{4-1} Fractional factorial design	20
4.6 Pharmaceutical degradations.....	21
4.7 Chemical oxygen demand (COD).....	21
4.8 Determination of hydrogen peroxide	22
4.9 Total organic carbon (TOC).....	23
4.10 Fluorescence analysis	23
4.11 PARAFAC model	24
4.12 MCR-ALS model.....	25
4.13 Partial Least Squares Regression (PLSR).....	26
4.14 Data treatment.....	26
4.15 HPLC analyses.....	26

4.16 Figures of Merit	27
4.17 Guideline.....	28
5 RESULTS AND DISCUSSION	29
5.1 Hydrogen peroxide production	29
5.2 Design of Experiments	30
5.3 2^{4-1} fractional factorial design	30
5.4 Central composite design	31
5.5 Degradation of the compounds	35
5.6 Fluorescence spectra	35
5.6.1 <i>Regression methods from chemometric methods and HPLC</i>	35
5.7 Application of the best model	38
5.7.1 <i>Ibuprofen results</i>	38
5.7.2 <i>Naproxen results</i>	40
5.7.3 <i>Mixture results</i>	41
5.8 HPLC results	44
5.9 TOC results	45
6 CONCLUSIONS.....	47
7 REFERENCES.....	48

ABBREVIATION LIST

Abreviation	English Term	Portuguese Term
ALS	Alternating Least Squares	Quadrados Mínimos Alternantes
ANOVA	Variance Analysis	Análise de Variância
AOPs	Advanced Oxidation Processes	Processos Oxidativos Avançados
BDD	Boron Doped Diamond	Diamante Dopado com Boro
CCD	Central Composite Design	Planejamento Composto Central
COD	Chemical Oxygen Demand	Demanda Química de Oxigênio
CORCONDIA	Core Consistency Diagnostic	Diagnóstico de Consistência de Núcleo
DC	Direct current	Corrente Contínua
DOE	Design of Experiments	Planejamento Experimental
EAOPs	Electrochemical Advanced Oxidation Processes	Processos Oxidação Eletroquímica Avançados
EEM	Excitation-Emission Matrix	Matriz de Excitação e Emissão
EF	Electro-Fenton	Eletro-Fenton
EV	Explained Variance	Variância Explicada
HPLC	High Performance Liquid Chromatography	Cromatografia Líquida de Alta Performance
IC	Inorganic Carbon	Carbono Inorgânico
IBU	Ibuprofen	Ibuprofeno
LOF	Lack of Fit	Falta de Ajuste
MCR-ALS _{un}	MCR-ALS with unfolded tensor	MCR-ALS com tensor desdobrado
MCR-ALS _{$\lambda=242$}	MCR-ALS with single matrix	MCR-ALS com uma matrix
MIX	Mixture	Mistura
NAP	Naproxen	Naproxeno
NSAID	Nonsteroidal Anti-Inflammatory Drugs	Medicamentos Anti-Inflamatórios não Esteroidais
PARAFAC	Parallel Factor Analyses	Análise de Fatores Paralelos
PLSR	Partial Least Square Regression	Regressão por Quadrados Mínimos Parciais
R	Correlation Coefficient	Coefficiente de Correlação
RMSE	Root Mean Square Error	Raiz Quadrática Média do Erro
RMSEC	Root Mean Square Error of Calibration	Raiz Quadrática Média do Erro de Calibração
RMSEP	Root Mean Square Error of Prediction	Raiz Quadrática Média do Erro de Previsão
RSM	Response Surface Methodology	Metodologia de Superfície de Resposta
SSE	Sum of Squared Error	Soma dos Erros Quadráticos
SVD	Singular Value Decomposition	Decomposição de Valores Singulares
TC	Total Carbon	Carbono Total
TOC	Total Organic Carbon	Carbono Orgânico Total

FIGURE LIST

Figure 1: Possible source and pathways for the occurrence of pharmaceuticals in aquatic environment.....	4
Figure 2: Naproxen structure.....	6
Figure 3: Ibuprofen structure.....	6
Figure 4: Graphic representation of the PARAFAC decomposition.....	14
Figure 5: Electrochemical cell used to degrade the solutions with BDD anode.	19
Figure 6: Electrochemical system: (A) Solution, (B) magnetic stirrer plate, (C) peristaltic pump, (D) electrochemical cell and (E) power supply.	20
Figure 7: Scheme of a tensor X built with the matrices recorded for each sample.....	24
Figure 8: Augmented matrix obtained by unfolding the tensor X.	25
Figure 9: Single matrix recorded at 242 nm excitation wavelength	26
Figure 10: Accumulation of H ₂ O ₂ during the time in the absence of Fe ²⁺	29
Figure 11: Pareto chart of the standardized effects.	31
Figure 12: Contour plot and response surface plot of the %COD removal as function of Na ₂ SO ₄ concentration and applied density of current, iron (II) concentration fixed at 30 mg L ⁻¹	34
Figure 13: Correlation between the measured and predicted values by the models. PARAFAC model IBU (A) and NAP (B), MCR-ALS model unfolded tensor IBU (C) and NAP (D), MCR-ALS $\lambda=242$ nm. NAP (E) and IBU (F), PLSR model IBU (G) and NAP (H). Calibration set (●), validation set (■).....	36
Figure 14: Norm of the fluorescence intensity over the time.....	39
Figure 15: Resolution of MCR-ALS for degradation of IBU. (A) Surface 3D of the fluorescence spectra through the time, (B) Recovered pure spectra of the estimated compounds. (C) Relative concentrations of the estimated compound. (D) Concentration predicted by the model.	39
Figure 16: Norm of the fluorescence intensity during the time.	40
Figure 17: Resolution of MCR-ALS for degradation of NAP. (A) Surface 3D of the fluorescence spectra through the time, (B) Recovered pure spectra of the estimated compounds. (C) Relative concentrations of the estimated compound. (D) Concentration predicted by the model.	41
Figure 18: Norm of the fluorescence spectra for the mixture.	42

Figure 19: Resolution of MCR-ALS for degradation of MIX. (A) Surface of the fluorescence spectra through the time, (B) Recovered pure spectra of the estimated compounds. (C) Relative concentrations of the estimated compound. (D) Concentrations predicted by the model.	43
Figure 20: Chromatography runs for aliquots taken from IBU (A and D), NAP (B and E) and MIX (C and F). Above are shown just the first and final aliquot, below there are all the aliquots taken from each degradation.....	44
Figure 21: Measured versus Predicted values of IBU and NAP concentrations estimated by MCR-ALS and HPLC. IBU degradation (A), NAP degradation (B) and MIX degradation (C and D).....	45
Figure 22: Total carbon organic removal, values are given in percentage. IBU (left side), NAP (middle) and MIX (right side).....	46

TABLE LIST

Table 1: Levels studied for each variable during the fractional factorial design.	20
Table 2: Overall of the methods and analyses.....	28
Table 3: Experimental matrix with coded, decoded factors and response.	30
Table 4: Experimental matrix with coded and decoded variables and response.....	32
Table 5: Regression coefficients and errors of the quadratic model.	32
Table 6: ANOVA of quadratic model.....	33
Table 7: Calibration parameters obtained for the methods PARAFAC, MCR-ALS and HPLC using standards.....	36

ABSTRACT

GABRIEL, Wesley Lira, M.Sc., Universidade Federal de Viçosa, February, 2018. **Electrochemical degradation of ibuprofen and naproxen using electro-Fenton process monitored by fluorescence and chemometric methods.** Advisor: Reinaldo Francisco Teófilo.

The use of fluorescence spectra and chemometric methods to monitor the electrochemical degradation of the drugs ibuprofen (IBU) and naproxen (NAP) using electro-Fenton process with boron-doped diamond (BDD) is the aim of this work. The variables of the degradation process were studied and optimized using design of experiments. Percentage of chemical oxygen demand removal was used as response in the design of the experiments. The results of the central composite design showed that the best conditions to perform the degradation were 60 mA cm⁻² of current density, 5500 mg L⁻¹ of Na₂SO₄ as support electrolyte and 30 mg L⁻¹ of Fe²⁺ as catalyst. Solutions of 30 mg L⁻¹ of the drugs were degraded, and aliquots were taken during 1h. TOC removal, fluorescence spectra, and HPLC were used to evaluate the degradation solutions of IBU, NAP and the mixture of the compounds (MIX). The fluorescence spectra were treated with chemometric methods, *i.e.*, parallel factors analysis (PARAFAC), multivariate curve resolution with alternating least squares (MCR-ALS) and partial least squares regression (PLSR). Models were built for each method and compared. The best fit was obtained with MCR-ALS method using fixed excitation wavelength (242 nm), and emission spectra scanned from 260 to 410 nm. The MCR-ALS was capable of recovering the pure emission spectra of the drugs and some byproducts generated. Also, the concentrations profiles of each compound were obtained. The fluorescence spectra of the compounds decreased significantly in less than 1 hour, which suggests a possible reduction of the toxicity of the solution. Results of separation and quantification obtained by HPLC with fluorescence detection were compared to the results obtained with MCR-ALS and fluorescence. Correlations high than 0.99 were achieved demonstrating that fluorescence spectroscopy associated with MCR-ALS method can substitute HPLC-fluorescence analysis in this application. Percentages of TOC removal were 77%, 65% and 63% to IBU, NAP, and MIX solution, respectively. The degradation process studied was efficient, and the monitoring method employing fluorescence and MCR-ALS showed to be fast, adequate and reliable.

RESUMO

GABRIEL, Wesley Lira, M.Sc., Universidade Federal de Viçosa, fevereiro de 2018. **Degradação eletroquímica de ibuprofeno e naproxeno usando processo eletro-Fenton monitorado por fluorescência e métodos quimiométricos.** Orientador: Reinaldo Francisco Teófilo.

O uso de espectros de fluorescência e métodos quimiométricos para monitorar a degradação eletroquímica dos fármacos ibuprofeno (IBU) e naproxeno (NAP) utilizando processo eletro-Fenton com diamante dopado com boro (BDD) é o objetivo deste trabalho. As variáveis do processo de degradação foram estudadas e otimizadas empregando planejamentos experimentais. A resposta usada nos planejamentos foi a remoção da demanda química de oxigênio. Os resultados do planejamento composto central mostraram que as melhores condições para realizar a degradação foram densidade de corrente de 60 mA cm^{-2} , 5500 mg L^{-1} de Na_2SO_4 como eletrólito suporte e 30 mg L^{-1} de Fe^{2+} como catalisador. Soluções de 30 mg L^{-1} dos fármacos foram degradadas e alíquotas foram retiradas durante 1h. O monitoramento das degradações das soluções de IBU, NAP e da mistura dos compostos (MIX) foi realizado empregando remoção de carbono orgânico total (TOC), espectros de fluorescência e HPLC. Os espectros de fluorescência foram tratados com métodos quimiométricos, *i.e.*, análise dos fatores paralelos (PARAFAC), resolução multivariada de curvas com quadrados mínimos alternantes (MCR-ALS) e a regressão com quadrados mínimos parciais (PLSR). Modelos foram construídos para cada método e comparados. O melhor ajuste foi obtido com o método MCR-ALS fixando o comprimento de onda de excitação em 242 nm e com emissão obtida entre 260 e 410 nm. O MCR-ALS foi capaz de recuperar os espectros puros dos fármacos e de alguns subprodutos formados além dos perfis de concentração de cada um. O sinal de fluorescência dos compostos diminuiu significativamente em menos de 1 hora, o que sugere uma diminuição da toxicidade da solução. Resultados das separações e quantificações obtidos usando o HPLC com detecção de fluorescência foram comparados com os resultados obtidos usando fluorescência e o método MCR-ALS. Correlações superiores a 0.99 foram encontradas, demonstrando que a espectroscopia de fluorescência aliada ao método MCR-ALS é capaz de substituir as análises por HPLC-fluorescência nesta aplicação. As porcentagens de remoção de TOC foram 77%, 65% e 63% para as soluções de IBU, NAP e MIX, respectivamente. O processo de degradação estudado foi eficiente e o método de monitoramento empregando fluorescência e MCR-ALS se apresentou rápido, adequado e confiável.

1 INTRODUCTION

The large consumption of human and veterinary pharmaceuticals have been a concern in the scientific community around the world. The amount produced is reaching quantities quite similar to those of pesticides and other organics pollutants. The pharmaceutical residues are biologically active and can enter by different ways in the environment, such as manufacture emissions, disposal of used and expired medicines, human and animal excretion and direct discharge of aquaculture products (GENTILI, 2007).

Pharmaceutical compounds have been detected in different quantities in the environment, being found in soil, water, and air. The occurrence has brought them to the group of emerging contaminants. These contaminants can be originated from different sources, which might include anthropogenic activities and natural occurrence. The term of emerging contaminants is related to the potential of these compounds to cause risk to ecosystem and human health, however; they are not included yet into monitoring programs and have no specific legislation for them (GENTILI, 2007; KÜ, 2009a; MONTAGNER et al., 2017). Among the pharmaceutical compounds that are emerging contaminants, the group of nonsteroidal anti-inflammatory drugs (NSAIDs) has received particular attention because they are most frequently detected, and their environmental distribution is widespread. Ibuprofen and naproxen are part of the most NSAIDs consumed in the world. Both compounds have been taken for treatment of pain and fever, and their detection in aquatic bodies have been reported in many papers in different concentrations (FENG et al., 2013; HEBERER, 2002; ISIDORI et al., 2005; MADHAVAN; GRIESER; ASHOKKUMAR, 2010; RICHARDSON; TERNES, 2017).

Most of the pharmaceutical compounds are detected in concentrations that range from ng L^{-1} to $\mu\text{g L}^{-1}$. It might seem to be small quantities, but the principal effect is related to the synergetic interactions with other pharmaceuticals and chemical substances in the aquatic environment (SODRÉ; LOCATELLI; JARDIM, 2010).

Because of the low concentrations of these compounds, conventional water treatments are not able to eliminate these compounds, which brings the need of advanced technologies that are capable of detecting and destroying these compounds from the environment. Advanced oxidative process (AOPs) are one of the most promising technologies developed in the last years. The AOPs are based on the generation of hydroxyl radicals ($\bullet\text{OH}$), which are excellent oxidative species. They can mineralize partial or completely organic compounds present in the reactional medium to CO_2 and

H₂O. The versatility of the AOPs is also enhanced by the fact that they offer different possibilities for radical production, thus allowing better compliance with the specific treatment requirements (ANDREOZZI, 1999). The generation of hydroxyl radicals can be performed direct and indirect through electrochemical process. In the first case, a current is applied in an anode and water molecule is broken leading to the formation of the radical, this process is known as homogenous process. The indirect generation, also known as heterogeneous process, is based on the combination of oxidative agents, such as O₃, H₂O₂, and catalyst (FENG et al., 2013). A variation of the AOPs is the electrochemical advanced oxidative processes (EAOPs). In these processes, the combination of homogeneous and heterogeneous processes is performed to enhance the generation of hydroxyl radical. Some examples of EAOPs are the electro-Fenton and photoelectron-Fenton processes (BRILLAS; SIRÉS; OTURAN, 2009).

The degradation of organic molecules can generate many byproducts. Being necessary methods and techniques that are able to monitor the profile degradation of the compounds. Fluorescence spectroscopy is a powerful technique that shows high sensitivity and selectivity. Since not all molecules have fluorescence characteristic, the study of target molecules using the technique shows excellent advantages. However, problems related to spectral overlapping can be faced in degradation studies. In general, for determination of an analyte with the problem presented, it would require many steps of extraction and separation, which take too much time, high reagent consuming and high cost of operations. Chemometric methods can be used as a great alternative to solve this type of problem because they are non-destructive, fast and environmentally friendly.

Two widely used chemometric methods for spectral resolution are the Parallel factor analyses (PARAFAC) and multivariate curve resolution with alternating least squares (MCR-ALS). Both methods are able to solve mathematically overlapping signals and extract chemical relevant information from the instrumental data of a mixture of components. Also, it is possible to determine the concentrations of the compounds with the relative concentrations recovered by the methods (BRO, 1997; OLIVIERI; ESCANDAR, 2014a).

2 OBJECTIVES

Main Objective:

- To use fluorescence spectra and chemometric methods to monitor the electrochemical degradation of the drugs ibuprofen (IBU) and naproxen (NAP) using electro-Fenton process with boron-doped diamond (BDD).

Specific Objectives:

- To study the conditions of the degradation system and optimize each variable using design of experiment.
- To degrade IBU, NAP and a mixture (MIX) of both using the optimized system.
- To evaluate the degradation of the solutions using fluorescence, HPLC and total organic carbon (TOC).
- To extract information of the fluorescence spectra using chemometric methods PARAFAC, MCR-ALS and partial least square regression (PLSR).
- To compare the HPLC analysis with the results of the fluorescence spectra treated with the best chemometric model.

3 LITERATURE REVIEW

3.1 Occurrence of pharmaceutical in water

In the recent years, the occurrence of active pharmaceutical compounds has been detected and became one of the most issues in environmental chemistry. The principal form of entrance of these compounds is based on anthropogenic activities. Every year, a large number of pharmaceutical compounds are consumed around the world, and significant unused overtime drugs for human and veterinary activity are released into environment continuously (FENG et al., 2013).

The conventional wastewater treatment is not able to eliminate these compounds due to their high or partial solubility in water. Also, they are very resistant to biological and conventional chemical process degradation (HEBERER, 2002). Therefore, the remains have great ability to reach the environment, which can get into aquatic bodies and potable water (Figure 1).

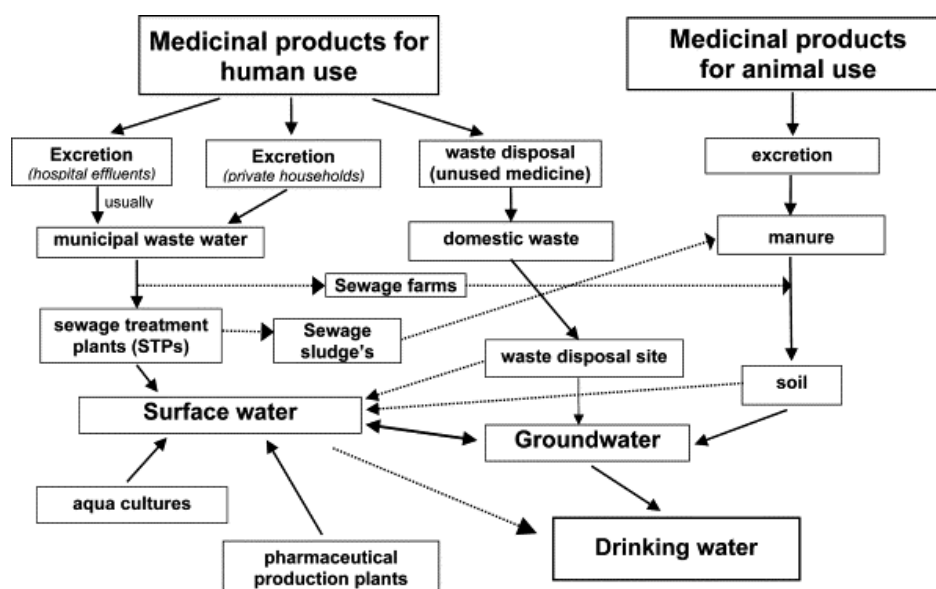


Figure 1: Possible source and pathways for the occurrence of pharmaceuticals in aquatic environment (HEBERER, 2002).

Studies have shown that the concentrations of pharmaceutical in surface water are in the order of ng L^{-1} and $\mu\text{g L}^{-1}$, however; it can change from countries around the world (KÜ, 2009b).

The presence of the drugs in drinking water may cause some effects that seem to be negligible. The amount of pharmaceutical compounds detected in water is much less than the dosages used in adult therapy. Therefore, questions related to environmental pollution are in many cases more important than questions related to toxicology and pharmacology of the compounds. However, some assumptions such as the effect of these

dosages for children, fetuses, babies, healthy adults and older adults have to be considered. Also, the dosage of a single compound is different from a mixture (CHRISTENSEN, 1998; KÜ, 2009b).

3.2 Emerging Contaminants

Emerging contaminants or simply contaminants of emerging concern are defined as naturally occurring, manufactured or humanmade chemicals or materials that have been discovered or are suspected present in the environment whose toxicity or persistence are likely to significantly alter the metabolism of living being (SAUVÉ; DESROSIERS, 2014).

The criteria for environmental quality is related to the emerging contaminants. The more a new compound begins to cause concern to the society, the more studies are carried out about it. However, in the case of the emerging contaminants, most of the compounds included in this group has no environmental guidelines to ensure adequate protection (SAUVÉ; DESROSIERS, 2014).

The focus of the discussion about the “emerging” term is based on the definition that brings not only the real mean of it, which can fail at some point. The emerging term has to be associated with chemical classes, types, effects, and mechanism of actions of the compounds. For each of the dimensions cited, it comes with a different perspective on how the compounds can affect living being (DAUGHTON, 2004).

The emerging contaminants can include many types of compounds, such as pesticides, pharmaceutical and personal care products, fragrances, plasticizers, hormones, flame retardants, nanoparticles, perfluoroalkyl compounds, chlorinated paraffin, siloxanes, algal toxins and various trace elements including rare earths and radionuclides (SAUVÉ; DESROSIERS, 2014).

The persistence and bioaccumulation of these compounds in the environment bring an increasing problem that affects a prerequisite for good health of human.

The presence of drugs in the environment has received some attention in the last fifteen years. They are considered emerging pollutants in waterbodies and still are unregulated or undergoing to regularization process (KÜ, 2009a; RIVERA-UTRILLA et al., 2013). The presence of these compounds in the environment is attributed to personal hygiene products, pharmaceutical industry waste, hospital waste and therapeutic drugs. Many studies have shown the presence of pharmaceuticals in water, most of these drugs are antibiotics, antihypertensive and non-steroidal anti-inflammatory. Also, some

hormones have been detected in trace levels (BOGER et al., 2015; CASTENSSON et al., 2009; FENG et al., 2014; RENOVATO, 2008).

In this context, many studies have been carried out to improve the wastewater treatment plants to contribute to the environment. These studies are based on new technologies, mainly chemical, with methods that can destroy and/or determine these compounds in surface water (BOGER et al., 2015; ZANIN et al., 2013).

3.3 Naproxen and Ibuprofen

Naproxen or (+)-(S)-2-(6-methoxynaphthalen-2-yl) propanoic acid is an anti-inflammatory agent with analgesic and antipyretic properties. The drug is commonly commercialized as a sodium salt. It is widely used for the treatment of rheumatoid arthritis and other rheumatic or musculoskeletal disorders (KANAKARAJU et al., 2015). The compound is chemically classified as a nonsteroidal anti-inflammatory drug (NSAID), and it can be used for both human and veterinary treatment.

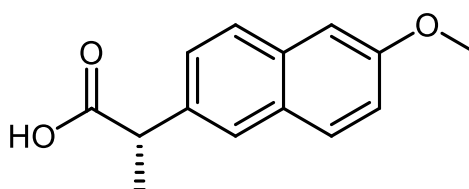


Figure 2: Naproxen structure.

Ibuprofen is also part of the NSAID group; its chemical name is 2-[3-(2-methylpropyl)phenyl] propanoic acid. It is prescribed for treatment of pain relief, fever, muscles, and toothaches (MADHAVAN; GRIESER; ASHOKKUMAR, 2010).

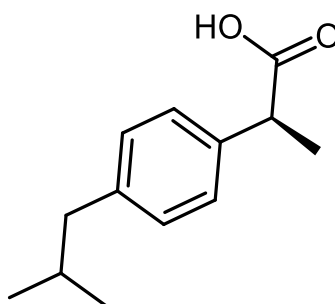


Figure 3: Ibuprofen structure.

Both compounds have been detected in wastewater treatment facilities and surface water. The persistence of these compounds became a topic that concerns modern societies. Because of the vast number of pharmaceutical compounds consumed around the world, these substances have been found in the environment. The reason is related to improper disposal of unused medicines. The way they reach in the environment can be

by human and animal excrement, flushed down via toilet and waste disposal site (FENG et al., 2013).

Studies have shown the detection of the compounds in concentrations that range ng L⁻¹ to µg L⁻¹. Naproxen has high acute toxicity, but the by-products after photo-degradation were shown to be more toxic than itself (ISIDORI et al., 2005). For biological degradation of ibuprofen, the toxicity of the by-products was shown to be quite similar to the original compound (ROBERTS; THOMAS, 2006). The main detected intermediates for ibuprofen degradation were phenol and 1,4-benzene carboxylic acid, also small molecular acids including 2-hydroxyl-propanoic acid, hydroxyl-acetic acid, pentanoic acid, and malonate (ZHAO et al., 2009).

Because of the massive consumption of these two compounds by the population, the significant challenge is the need of more powerful environmentally friendly technologies that are capable of detecting even more low concentrations and able to destroy these compounds entirely from the environment; and therefore, minimize the risks to human health and ecosystems.

3.4 Advanced Oxidation Processes (AOPs)

The advanced oxidation processes are characterized by the chemical oxidation reaction with hydroxyl radical ($\cdot\text{OH}$), a specie very reactive and not very selective. The radical can promote the oxidative degradation of many organic compounds due to its high reduction potential ($E^\circ = +2,73 \text{ V}$) which is higher than the other oxidative species used in conventional treatment, such as ozone, fluorine, and chlorine (MELO et al., 2009).

The chemical oxidation aims to mineralize the contaminants present in the sample to carbon dioxide, water, and inorganic compounds or to promote the break of these contaminants into harmless molecules.

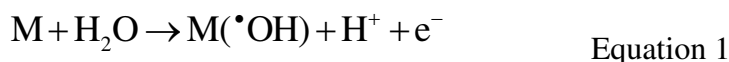
The hydroxyl species can be generated from high oxidative reagents, such as H₂O₂ and O₃. A good strategy that can be used to increase the efficiency of the process is the combination of ultraviolet or visible radiation and the presence of a catalyst. The mechanisms of interaction with the contaminants can be very different from each species. It has been observed that aromatic and unsaturated compounds react with electrophilic addition and form organic radicals that promote oxidative chain reactions that lead to mineralization (ANDREOZZI, 1999; MELO et al., 2009).

Among the AOPs, different methods can be identified according to the type of process, such as wet oxidation, ozonation, Fenton process, sonolysis, homogeneous ultraviolet irradiation, heterogeneous photocatalysis using semiconductors, radiolysis and

a great number of electric and electrochemical methods (BRILLAS; SIRÉS; OTURAN, 2009; MELO et al., 2009).

In the last decade, a variation of the AOPs has been studied, so-called EAOPS, which is the electrochemical process. The electrochemical process includes anodic oxidation, in which an anode is used to promote the production of heterogeneous $\cdot\text{OH}$ in the surface of the anode. Processes such as electro-Fenton, photoelectron-Fenton, and sonoelectrochemistry also are used. In these ones, homogeneous $\cdot\text{OH}$ is generated into the solution. An advantage of the EAOPS is the possibility to combine the different types process to increase the generation of $\cdot\text{OH}$ (SIRÉS et al., 2014).

The radical $\cdot\text{OH}$ produced from water in the anode surface (Equation 1) are transferred directly to the solution. The generation can be performed by the water oxidation in the surface of different materials, such as PbO_2 , SnO_2 , Pt, boron doped-diamond (BDD) and many others (ZANIN et al., 2013).



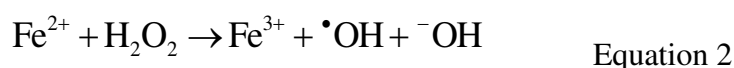
where $\text{M}(\cdot\text{OH})$ is the hydroxyl radical adsorbed in the surface of the anode M.

BDD has commonly been used as an anode because of the advantages presented by this material. The BDD anode is the most potent non-active electrode known, and it is considered the most suitable anode for treatment of organic compounds by anodic oxidation. The high quality of the electrode is related to the wide potential window in aqueous medium, the corrosion stability in aggressive medium, inert surface with low adsorption properties and strong tendency to resist deactivation (MARSELLI et al., 2003; PANIZZA; CERISOLA, 2009; RIVERA-UTRILLA et al., 2013).

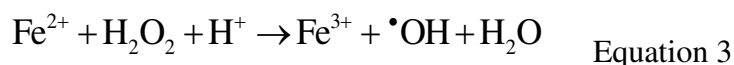
3.5 Fenton process

H.J.H Fenton described the Fenton's chemistry in 1876 when tartaric acid was destroyed by a mixture of Fe^{2+} and H_2O_2 . However, only in 1894, the Fenton's chemistry was widespread after an in-depth study published about the reaction between the reagents and the tartaric acid. Since then, the Fenton's reaction has been used as one of the most effective methods to destroy organic pollutants (BARBUSIŃSKI, 2009; BRILLAS; SIRÉS; OTURAN, 2009).

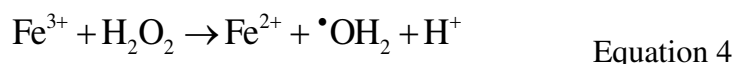
The oxidation using Fenton's reaction is performed by the production of reactive oxidizing species, hydroxyl radicals ($\cdot\text{OH}$). The mechanism more accepted to this reaction is given by the Equation 2:



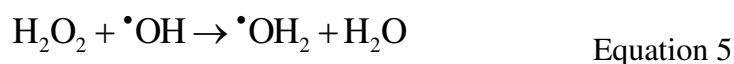
A good aspect to note is that the best condition for the reaction is dependent on the pH medium, which is given within pH around 2.8 to 3. Thus, the reaction also can be described by Equation 3:



The pair $\text{Fe}^{2+}/\text{Fe}^{3+}$ acts as catalyst in the reaction. A simple quantity of Fe^{2+} is needed to the development of the reaction since the reagent is regenerated in the medium through the process called Fenton-like (Equation 4):

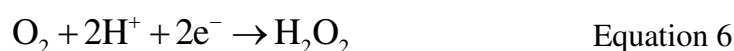


It is important to know that the stoichiometry must be satisfied. Otherwise, parallel reaction can occur and decrease the generation of reactive species. The amount of hydrogen peroxide in excess can promote the production of a radical that is much less reactive than the $\cdot\text{OH}$ (Equation 5):



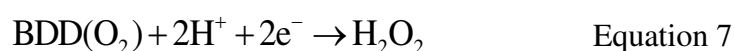
The effect of the excess of H_2O_2 was demonstrated to be adverse in the degradation of organic compounds such as herbicides and aquatic effluents; therefore, the amount of this reagent has to be adequate (PUPO NOGUEIRA et al., 2007).

Taking the advantages of the EAOPs, H_2O_2 can be successfully produced in a divided or undivided electrolytic cell from the two-electron reduction of oxygen gas (Equation 6), which can be directly injected into the solution as pure gas or bubbled air (BRILLAS; SIRÉS; OTURAN, 2009).



One of the advantages of the Fenton process is that it can be combined with other AOPs processes to increase the capacity of the $\cdot\text{OH}$ production, and so, the capacity to eliminating pollutants in the medium. Boron-doped diamond has been used associated with the Fenton process to increase oxidation of the compounds; this method is usually known as electro-Fenton process.

The electro-Fenton process, which can be defined as an electrochemically assisted Fenton's process, has been known as one of the most popular techniques among the EAOPs. The combination of BDD and the Fenton's reaction are given by the Equations 2 and 7 (CRUZ-RIZO et al., 2017).



The main advantages that this combination presents compared to the classical Fenton's reaction is the in-site production of H₂O₂ that eliminate risks associated with transportation, storage, operation and cost related to this reagent. Also, high mineralization of organic compounds can be achieved due to the continuously electro-generation of the catalyst Fe²⁺; no sludge is formed during the process and secure control of the parameters (SOPAJ et al., 2016).

Many papers can be found with applications of the method electro-Fenton combined with BDD as anode. The method was used to treat tannery wastewater in industrial residues (CRUZ-RIZO et al., 2017), in the mineralization of the antibiotic sulfamethazine (SOPAJ et al., 2016), in the degradation of the antihypertensive losartan and herbicides (MURATI et al., 2012; SALAZAR et al., 2016) and many others. The applications show the efficiency and versatility of the method.

3.6 Fluorescence spectroscopy

Fluorescence is a spectrochemical method of analysis where the molecules of an analyte are excited by irradiation at a specific wavelength and emit radiation in a different wavelength. The emission spectrum can provide qualitative and quantitative information about the analyte of interest. Once the molecules are in the excited state, relaxation can occur via several processes. Fluorescence is one of these processes that result in the emission of light (SKOOG et al., 2011).

The reason for the phenomenon of fluorescence is the quantum yield, which is the ratio of the number of molecules that presents fluorescence characteristic and the number of molecules that were excited. Molecules that fluoresce intensely, present high quantum yield at specific conditions. Some factors that influence the process are the pH, temperature, stiffness of the molecule, present of unsaturation in the structure of the molecule and the solvent.

The intensity of the fluorescence (I_f) is directly proportional to the intensity of the excitation beam (I_0), the absorbance (ϵbc) and the quantum yield of the specie (ϕ_f), which are defined by Equation 8:

$$I_f = K_f I_0 \Phi_f \epsilon bc \quad \text{Equation 8}$$

where K_f is a constant that is function of the instrumental response and other instrumental parameters. Due to the direct proportionality of the I_f and I_0 , sensitivity, and limits of detection can be improved based on this characteristic (TREVISAN, 2003).

The radiation sources for fluorescence instruments are in general more powerful than in absorbance instruments. The radiant potency emitted is directly proportional to

the source intensity, on the other hand; absorbance is related to the ratio of the potencies, which is independent of the source intensity. Thus, the fluorescence technique presents sensitivity higher than absorbance techniques (SKOOG et al., 2011).

Interferences can occur when fluorescence spectra are being recorded. A very common interference is the scattering effects; mainly Rayleigh and Raman scatter which must be avoided. There are several ways to handle scattering effects, some involve instrumental processes, such as the use of filters or polarizers, others use algorithms that are able to eliminate the region where the scattering occurs, or only switch the area for mathematics values (BAHRAM et al., 2007).

Fluorescence intensity can decrease by the interaction of the excited state of the fluorophores present in the sample. This phenomenon is known as “quenching” and can occur when mixtures of fluorophores are being analyzed. Besides, the solvent can interfere and promote quenching. The concentration of the fluorescent species can generate two types of quenching: self-quenching, which is when the excited molecules transfer energy to the molecules of the solvent leading to a decrease of the intensity of the fluorescence. The other type is self-absorption that occurs when there is overlapping of excitation and emission wavelengths, in this case, other molecules can absorb the radiation that is emitted by other molecules and only a few parts of the radiation reaches the detector (SKOOG et al., 2011; TREVISAN, 2003).

There are some ways to eliminate quenching phenomenon, such as mathematic models, separation of the mixtures or simply work with diluted solutions. In last one, it can decrease the detection and quantification limits.

Excitation-Emission Matrix (EEM) can be generated by the excitation and emission spectra of an analyte. The matrix is obtained by fixing an excitation wavelength and performing an emission scanning in a specific range. It is possible to perform the contrary, fixing an emission wavelength and scanning the excitation. EEMs are generated in two independent dimensions, one with the excitation profile and the other one with the emission profile. The EEM provides information on the number of fluorophores present in the sample and their abundance (ANDERSEN; BRO, 2003).

3.7 High-Performance Liquid Chromatography (HPLC)

Chromatography is a technique that allows separating the components of a mixture based on their difference of velocity through a stationary phase by a mobile phase that can be liquid or gas (SKOOG et al., 2011). The chromatography techniques are deeply applied in the separation of complex mixtures, such as biological samples, chemical

components, natural products, air and many others. Separation by HPLC depends on some parameters of the stationary and mobile phase, such as polarity, flow rate, pH, type and nature of the phases, pressure, temperature and the detector type (SAHU et al., 2018).

In HPLC analyses the mobile phase is a liquid solvent or a mixture of solvents that will carry the analytes through a column containing the stationary phase. The separation is performed based on the interactions between the analytes and the stationary phase. Analytes that have high interaction with the stationary phase will remain in the column in different time from those whose interaction is not high. The detection can be made by different types of detectors. The most applied is the ultraviolet/visible detector, but there are more types available, such as fluorescence, refraction index and electrochemical (VIEIRA, P. C.; CASS, Q. B.; DEGANI, 1998).

The technique was used to identify the byproducts in the degradation of ibuprofen in photocatalytic studies (MADHAVAN; GRIESER; ASHOKKUMAR, 2010). Also, Coria et al. used the technique to monitor the concentration of naproxen and its byproducts after a electro-Fenton process (CORIA et al., 2016).

3.8 Chemometrics

Chemometrics is an area of the chemistry that use mathematical, statistical and computational concepts to identify and extract relevant chemical information of the data, optimize parameters of the system in study and obtain the maximum information about the system (KOWALSKI, 1980).

3.8.1 Design of experiments

Design of experiments (DOE) allows to study the variables of a system and how these variables can influence the response in the study. It also permits to optimize each variable and achieve the best condition that will lead to the best result. There are many types of DOE, each one has proprieties that are adequate to specific type of problem that must be solved, and it is the role of the scientist to choose which one will be more suitable to solve the problem. The full factorial design, the fractional factorial design, and the central composite design are the common types of DOE that have been used lately (TARLEY et al., 2009).

In any experimental procedure, several experimental variables or factors may influence the result. A screening experiment can be performed to identify the experimental variables and interactions that have significant influence on the result, measured in one or several responses. In a screening study, the first and second order

interactions between the variables are obtained by full factorial and fractional factorial design. These experiments are chosen because they permit to study the system in only two levels for each variable, a level minus (-) and plus (+) describing the low and high level. If the combination of k factors are investigated at two levels, a factorial design will consist of 2^k experiments. Besides that, it is possible to include experiments at the mid value between the two levels, defined as level zero (0), which characterize the central point and repetition that allows determination of confidence intervals (LUNDSTEDT et al., 1998; TEÓFILO; FERREIRA, 2006).

After screening experiments, the significant factors are selected and can be analyzed by response surface methodology (RSM). The RSM is carried out in order to optimize the experiment. The optimization consists of finding the variables values that will lead to the best response. The RSM is built with linear and quadratic empiric models, which are obtained with specific design of experiments. A typical design of experiment for optimization in analytical chemistry is the central composite design (CCD).

A CCD consist of the combination of a full factorial or fractional factorial design, experiments at the central point, $x_i = 0$, and experiments situated on the axial points in which $x_i = \pm \alpha$ and $x_j \neq x_i = 0$, where $\alpha = \sqrt[4]{2^k}$. These points are situated on the axis of a co-ordinate system with distance $\pm \alpha$ from the origin. To perform experiments using CCD it is necessary to define the number of variables in the study (k), which factorial design will be employed and how many experiments in the central point will be performed. The number of experiments is given by $2^k + 2k + 1$ (TEÓFILO; FERREIRA, 2006).

3.8.2 Signal resolution methods

There are many methods in the literature for resolution signals, but the most common in chemistry is the parallel factor analyses (PARAFAC) and the multivariate curve resolution with alternating least squares (MCR-ALS). Both methods are very powerful tool for signals resolution due to their high efficiency, robustness, ability to process multiple samples and availability of a variety of constraints to be applied during the fit. The constraints normally ensure reaching physically interpretable results (ESCANDAR et al., 2014).

3.8.3 Parallel factor analyses

To model a three-way data array, a data matrix has to be available as a set of experimentally measured signals, such as EEM. The goal is to decompose the three-way array in trilinear terms and a residual array to fit the trilinear model. The decomposition of the data can be described by Equation 9:

$$x_{ijk} = \sum_{f=1}^F a_{if} b_{jf} c_{kf} + e_{ijk} \quad \text{Equation 9}$$

where, x_{ijk} is an element at the position ijk for i^{th} sample at j^{th} variable in the mode 2, and at k^{th} variable on mode 3, e_{ijk} is the residual, which are not accounted by the model. F is the number of factors for the model (MURPHY et al., 2013). a_{if} , b_{jf} , and c_{kf} are the elements of \mathbf{A} , \mathbf{B} and \mathbf{C} matrices (Figure 4). When fluorescence data is available, the columns in \mathbf{A} has the concentrations recovered for each fluorophore in the sample, \mathbf{B} and \mathbf{C} have the emission and excitation spectra, respectively. However, the data also can be pH values, elution times, reaction times, etc, i.e. each of the different instrumental channel which are experimentally accessible as digital points (MBOGNING et al., 2014; OLIVIERI; ESCANDAR, 2014b).

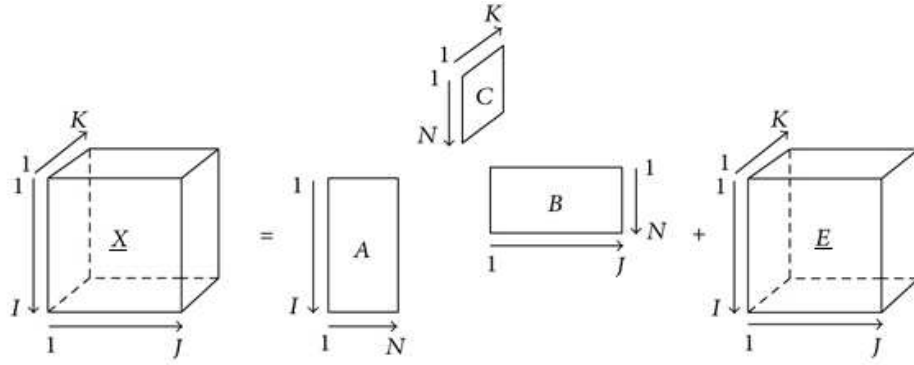


Figure 4: Graphic representation of the PARAFAC decomposition (ACAR; YENER, 2009)

There are several available algorithms that are able to decompose trilinear data. The most popular is parallel factor analysis (PARAFAC). The aim of the PARAFAC algorithm is to find the values of the parameters a_{if} , b_{jf} and c_{jf} by minimizing the sum of the squared errors (BRO, 1997):

$$SSE = \sum_{i=1}^I \sum_{j=1}^J \sum_{k=1}^K e_{ijk}^2 \quad \text{Equation 10}$$

The algorithm starts with the initial estimation of the parameters and then refines these initial values iteratively until the SSE is minimum. The parameters are not varied simultaneously in each iterative cycle of the algorithm but in an alternating manner. Once the first parameter is allowed to vary, the remaining are kept fixed. Then the second parameter is allowed to vary; the remaining are kept fixed, and so on. This procedure is known as alternating least-squares (ALS) (OLIVIERI; ESCANDAR, 2014b).

The main advantage of PARAFAC is that the solutions are often unique (TEN BERGE, 2004). The uniqueness property has immense consequences in multiway analytical calibration, because it provides this calibration with one of its main advantages, i.e., the possibility of quantifying analytes in samples containing unexpected constituents, even if these constituents are not in the calibration set, which is called “second-order advantage”. Uniqueness means that a unique solution exists for all parameters a_{if} , b_{jf} and c_{if} when the decomposition of a trilinear three-way array with PARAFAC is performed with the right number of components and the data is indeed trilinear (BRO, 1997; OLIVIERI; ESCANDAR, 2014b; SENA; TREVISAN, 2005).

Selecting the right number of components is sometimes too complicated, but it is essential to know that the right number of components should lead to a good fit of the model. There are statistical tests that can be carried out to indicate when the fit will be satisfactory. Three main ways of determining the correct number of components are: (1) split-half experiments, (2) judging residual fit and (3) analyzing the core consistency diagnostic, CORCONDIA.

The idea in the split-half analysis is to divide the data into two halves and then make a PARAFAC model on both halves. Due to the uniqueness of the PARAFAC model, one half will obtain the same results of the other half if the right number of compounds is chosen. To judge if two models are equal, one must remember the intrinsic indeterminacy in PARAFAC: The order and scale of a model may change if not fixed algorithmically. If a wrong number of components is chosen in the split-half analysis, there is a good chance that the two model will not be equal, due the differences in the sample (BRO, 1997; HARSHMAN; LUNDY, 1994).

The residual judging fit is based on the analysis of the Equation 10. The value for residual fit should decrease when increasing the number of components until it stabilizes at a particular value that will be considered optimal (OLIVIERI; ESCANDAR, 2014b).

Core consistency diagnostic is based on the following Equation 11:

$$\%CORCONDIA = \left(1 - \frac{\sum_{d=1}^F \sum_{e=1}^F \sum_{f=1}^F (g_{def} - t_{def})^2}{\sum_{d=1}^F \sum_{e=1}^F \sum_{f=1}^F t_{def}^2} \right) \times 100 \quad \text{Equation 11}$$

where g_{def} is the calculated element of the core using the PARAFAC model, defined by dimensions ($d \times e \times f$); t_{def} is the element of a binary array with zeros in all elements and ones in the super-diagonal and F is the number of factors in the model. In ideal

PARAFAC g_{def} is equal to t_{def} and, in this case, CORCONDIA will be equal to 100%. When a sequence of models are run with an increasing number of components, the CORCONDIA tends to start high (about to 100%) and drop significantly at the point when too many components are selected.

The PARAFAC method has been applied in many studies. The method was used in the exploration of essential oil using EEM (MBOGNING et al., 2014), in the determination of linezolid and application to pharmaceutical formulation (ABD et al., 2014), tracing dissolved organic matter in aquatic environments (STEDMON; MARKAGER; BRO, 2003), in the determination of polycyclic aromatic hydrocarbons in the presence of interferences (CAÑAS; RICHTER; ESCANDAR, 2014) and many other applications.

3.8.4 Multivariate curve resolution-alternating least squares

The multivariate curve resolutions are methods for signal preprocessing with the objective of solving mixture signals. They are based on the extraction of the main information of the pure components in a mixture system. It is capable of providing chemical information about the components present in system through a bilinear model decomposition. An experimental matrix $\mathbf{D}_{(i,j)}$ is decomposed in a product of matrices \mathbf{C} e \mathbf{S}^T that contains pure profiles of components, usually concentrations and spectra (DE JUAN; JAUMOT; TAULER, 2014; JAUMOT; DE JUAN; TAULER, 2015). The bilinear model can be described by the equation:

$$\mathbf{D} = \mathbf{C} \times \mathbf{S}^T + \mathbf{E} \quad \text{Equation 12}$$

where \mathbf{E} is the residual matrix that is not explained by the model.

The method MCR-ALS is one type of multivariate curve resolution that the iterative resolution of the Equation 12 is performed with the algorithm ALS. Two specific conditions have to be verified in order to use the MCR-ALS. Initially, the analytical signal has to obey the Lambert-Beer law, i.e., the signal has to have a linear relationship with the concentrations. The second condition is that the rank of the data matrix has to be equal to the number of species present in the mixture (MARÇO et al., 2014).

The number of components is estimated using the singular value decomposition algorithm (SVD). An experimental matrix with arbitrary dimension can be described by the product of three matrixes as follow:

$$\mathbf{X} = \mathbf{A} \times \mathbf{D} \times \mathbf{P}^T \quad \text{Equation 13}$$

The matrix $\mathbf{A} \times \mathbf{D}$ is defined as scores and hold the sample coordinates in the axis of the components. \mathbf{P} matrix holds the information of how the original variables are related to the components. This matrix is called loadings. The \mathbf{D} matrix is a diagonal matrix and carries information about the variance in each component. The number of components is obtained through the diagonal of the \mathbf{D} matrix. Usually, when there are active species in the matrix \mathbf{X} , the first values of \mathbf{D} are high and positive. When one of the first values is approximately zero, it indicates that the number of active species were achieved (FERREIRA et al., 1999).

Initial estimates in MCR-ALS can be concentration profiles or spectra. The simple rule is to start with initial guesses, which already obey the constraints that will be applied during the optimization. These initial estimates can come from previous knowledge about the system if available, such as the pure spectra of some of the components in the system. In case that there are no previous knowledge, there are methods that can help in the task of obtaining this initial information. A common denomination of these methods is pure variable selection methods. Some of the most widely known in simple-to-use self-modeling analysis, also called SIMPLISMA. The SIMPLISMA select the most different rows or columns in a single matrix or a multiset structure providing initial estimates of spectra or concentration profiles (DE JUAN; JAUMOT; TAULER, 2014).

Once the initial estimative is selected, the iterative optimization is started with the ALS algorithm. For each iterative cycle, the matrices \mathbf{C} and \mathbf{S}^T are recalculated in two steps using least squares, the calculation is performed under some constraints that are established initially. The main constraints applied in MCR-ALS are non-negativity, unimodality, and closure, all the constraints can be applied in the rows and columns and are responsible for giving shape to the row and column profiles in the bilinear model of the data. They are mathematical conditions and lead the MCR optimization process to the final solution; these conditions give the MCR-ALS the capacity to present “second-order advantage”, which is useful in many cases (MARÇO et al., 2014).

The quality of the MCR-ALS model is assessed by the percentage of lack of fit (%LOF) and the percentage of explained variance (%EV), these parameters are estimated by the equations:

$$\%LOF = 100 \times \sqrt{\frac{\sum e_{ij}^2}{\sum d_{ij}^2}} \quad \text{Equation 14}$$

$$\%EV = 100 \times \left(1 - \frac{\sum e_{ij}^2}{\sum d_{ij}^2} \right) \quad \text{Equation 15}$$

where, d_{ij} is an element of the experimental data matrix and e_{ij} is the related residual value obtained from the difference between the experimental data \mathbf{D} , and the reproduced data obtained by the MCR-ALS (JAUMOT; DE JUAN; TAULER, 2015).

3.8.5 Partial Least Squares Regression

The partial least squares regression (PLSR) is considered the most used regression method in multivariate calibration with first order data. The method has become a powerful tool for modeling multivariate data. The method present “first-order advantage”, which means that the method does not require accurate knowledge of all components present in the samples, and it is able to perform prediction of an analyte of interest even in the presence of interferences, as long as the interferences are also present in the calibration set (ROQUE; DIAS; TEÓFILO, 2017).

The PLS is calculated through computational algorithms. There are many PLS algorithms available in the literature, such as NIPALS, bidiagonal, SIMPLS and Kernel (DE JONG, 1993; LINDGREN; GELADI; WOLD, 1993). However, Martins et al. (2010) performed tests with some algorithm and concluded that the bidiagonal is the one which takes less time and it is the more intuitive (MARTINS; TEÓFILO; FERREIRA, 2010).

A bidiagonal algorithm is based on the decomposition of a matrix \mathbf{X} into three matrixes:

$$\mathbf{X} = \mathbf{URV}^t \quad \text{Equation 16}$$

where \mathbf{UR} is a matrix of scores and \mathbf{V} is a matrix of loadings.

The columns of \mathbf{U} and the rows of \mathbf{V}^t originate a new system of axis of the original matrix and are denoted as latent variables (h). The latent variables are orthogonal and bring decrescent information and complementary of the variance of the \mathbf{X} matrix. Typically, the first latent variables are able to rebuild the \mathbf{X} matrix with approximately 100% of the original information.

4 MATERIALS AND METHODS

4.1 Chemicals

All chemicals used in this work were of high-grade purity. Ibuprofen, naproxen (>99% pure) and acetonitrile of HPLC grade were purchased from Sigma-Aldrich. Sodium sulfate and iron (II) sulfate heptahydrate were supplied by Impex and Neon, respectively. Formic acid (>98% pure) was provided by Panreac. Mercury (II) sulfate was purchased from Dinâmica. Sodium oxalate (>99,9% pure) was provided by Merck and silver sulfate (>98% pure) by Cennabras. Solutions of the pharmaceuticals, sulfuric acid, and sodium hydroxide were prepared with ultrapure water.

4.2 BDD Anode

A BDD electrode was purchased from NeoCoat[®]-Electrodes. The BDD films were deposited on a monocrystalline silicon substrate with 60 mm of geometry, 2 mm of thickness and resistivity of 100 mΩ.cm. The thickness of the BDD coating was 2-3 μm, and the boron concentration on the substrate was 5000 mg L⁻¹.

4.3 Electrochemical cell

An electrochemical cell was used to degrade the solutions according to the cell built by Souza, T. S. et al. (SOUZA et al., 2016). The schematic cell is presented in Figure 5. The BDD anode (1) was fixed at the surface of stainless steel (2), the solution was kept in circulation through the entrance and exit channels (3), a stainless steel plate (AISI 304) was used as cathode (4) and the parts were united by threading the external part (6). Isolation of the system was done using a Viton[®] *O-ring* (5). The distances between the anode and cathode were 5 mm approximately. The silicon disk covered with BDD thin-film had an available geometrical area of 20 cm².

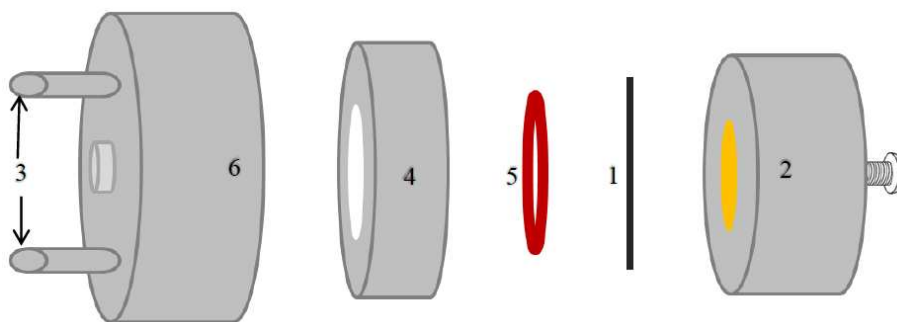


Figure 5: Electrochemical cell used to degrade the solutions with BDD anode.

4.4 Degradation system

For degradation of the compounds, a system was developed using a DC supply power. The voltage applied to the system was fixed at 50 V. All solutions in the study were placed in a beaker and were kept in circulation using a peristaltic pump. The solutions were stirred with a magnetic bar and were saturated with compressed air to the continuous production of peroxide hydrogen (FENG et al., 2013) during the degradation. Figure 6 shows the electrochemical system scheme.

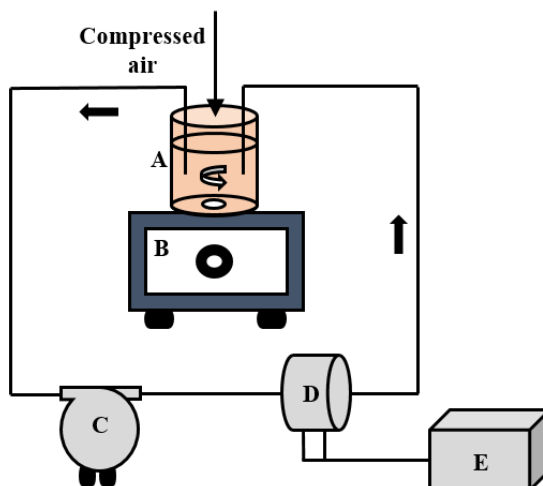


Figure 6: Electrochemical system: (A) Solution, (B) magnetic stirrer plate, (C) peristaltic pump, (D) electrochemical cell and (E) power supply.

4.5²₄¹ Fractional factorial design

A 2^{4-1} fractional factorial design with four experiments on central point was performed to investigate how the variables of the system could influence the process of degradation of the compounds. Table 1 shows the levels studied during the experiments.

Table 1: Levels studied for each variable during the fractional factorial design.

Variables	(-)	0	(+)
$j / \text{mA cm}^{-2}$	15	30	45
$[\text{Fe}^{2+}] / \text{mg L}^{-1}$	0	15	30
$[\text{Na}_2\text{SO}_4] / \text{mg L}^{-1}$	1000	3000	5000
Flow / L h^{-1}	2,5	4,0	5,5

j : current density; $[\text{Fe}^{2+}]$: Fe^{2+} concentration; $[\text{Na}_2\text{SO}_4]$: Na_2SO_4 concentration; Flow: solution flow.

The current density was studied during the experiments in order to know whether or not it can improve the process of degradation. The concentration of Na_2SO_4 was studied because the presence of an electrolyte in the solution can improve the efficiency of the degradation (CRUZ-RIZO et al., 2017). In the electron-Fenton reaction, the

concentration of iron(II) is mandatory, besides that high concentrations of it can generate parallel reactions (BARBUSIŃSKI, 2009). The flow of the solution was studied because it is expected that when the solution remains inside the electrochemical cell, more it will be in contact with the oxidant medium. Therefore, it is expected a high percentage of degradation using slow flow. The response (dependent variable) used in the experimental design was the percentage of chemical oxygen demand (COD).

The results from the fractional factorial design were used to perform the optimization of the system using response surface methodology.

All experimental design calculations were performed using spreadsheets according to Teófilo and Ferreira (TEÓFILO; FERREIRA, 2006).

4.6 Pharmaceutical degradations

After the system optimization, 400 mL of a solution containing the compounds were degraded in triplicate at the optimal conditions. Degradations were performed for 30 mg L⁻¹ of IBU and 30 mg L⁻¹ of NAP individually, and for a mixture containing 30 mg L⁻¹ of each one during 1h. Aliquots were taken at 0, 5, 10, 15, 20, 25, 30, 40, 50 and 60 min. Fluorescence spectra were acquired for studies of the degradation profile of the compounds using multivariate calibration. Also, total organic carbon and chromatography analyses were executed.

4.7 Chemical oxygen demand (COD)

The removal of chemical oxygen demand was used as response (dependent variable) in the design of experiments executed in this work. The Equation 17 shows the removal of chemical oxygen demand calculation.

$$\%COD = \frac{COD_0 - COD_f}{COD_0} \cdot 100 \quad \text{Equation 17}$$

where COD₀ and COD_f are the chemical oxygen demand in the beginning and the ending of the degradation, respectively.

The COD determination was performed according to the procedure used at Environmental and Sanitary Engineering Laboratory (LESA) at UFV – Minas Gerais, Brazil.

The procedure is described as following.

Digester solution: a mass of 1.022 g of K₂CrO₇ previously dried at 103 °C for 2h was weighted in a beaker, 33.3 g of HgSO₄ was added into the beaker, followed by 167

mL of concentrated H₂SO₄ and 500 mL of distilled water. The solution was homogenized and transferred to a flask of 1 L. The volume was completed with distilled water.

Catalyst solution: a mass of 10.210 g of Ag₂SO₄ was weighted in a beaker and diluted in 500 mL of concentrated H₂SO₄. The solution was transferred to a flask of 1L, and the volume was completed with concentrated H₂SO₄.

Standard solutions: a calibration curve was built with different concentrations of potassium biphthalate (KHC₈H₄O₄). A stock solution of 1500 mg L⁻¹ of COD was prepared weighting 0.6375 g of KHC₈H₄O₄, which was previously dried for 1h at 120 °C. The mass was diluted to a flask of 500 mL and completed with distilled water.

Standards were prepared in flasks of 25 mL from the stock solution in the concentrations: 0, 20, 40, 60, 80 and 100 mg L⁻¹.

Calibration curve: In appropriated tubes for COD, 2.5 mL of the standard was added, 1.5 mL of digester solution and 3.5 mL of catalyst solution. The tubes were sealed and heated in a digester at 150 °C for 2h. The analytical range for this curve was 0 – 100 mg L⁻¹. After two hours the tubes were removed from the digester and cooled for approximately 30 min. The analyses were made in a BioChrom spectrophotometer model S1200 Spectrawave at 420 nm, and the blank for the curve was distilled water. The calibration curve was built based on the linear relationship between the concentration of COD and absorbance of the samples.

For the degradation samples, the procedure was executed as described above, but the standard was replaced by the sample. The COD concentrations for the samples were obtained using the calibration curve and the absorbance measured for each sample.

4.8 Determination of hydrogen peroxide

The determination of hydrogen peroxide generated into the solution was executed without the presence iron (II) and any other target compounds. The accumulation was monitored during four hours in the presence of 5000 mg L⁻¹ of Na₂SO₄ and pH 3 with 45 mA cm⁻² of density of current, the volume of the solution was 400 mL. Aliquots were taken at 15, 30, 60, 90, 120, 180, 240 min. The concentration accumulated was determined for each aliquot by standard titration with potassium permanganate (KMnO₄) 0.02 mol L⁻¹.

The solutions for titration were prepared according to the following procedure:

A stock solution KMnO_4 0.02 mol L^{-1} was prepared weighting a mass of 1.5801 g and diluted into a flask of 500 mL. The solution was homogenized and heated for 25 min; then, it was filtered and cooled down until room temperature ($\sim 25 \text{ }^\circ\text{C}$).

A solution of sulfuric acid (H_2SO_4) 1:5 v/v was prepared in a flask of 200 mL.

The standardization of KMnO_4 was made weighing in an erlenmeyer 0.1000 g of sodium oxalate ($\text{Na}_2\text{C}_2\text{O}_4$) as a primary standard, which was previously dried for 2h. 10 mL of H_2SO_4 1:5 v/v and 25 mL of water were added into the erlenmeyer. The solution was heated until $60 \text{ }^\circ\text{C}$ and the titration was executed with KMnO_4 $4.0 \times 10^{-4} \text{ mol L}^{-1}$. The analysis was carried out in triplicate.

After the standardization, the titration was performed for the aliquots that were taken during the accumulation of hydrogen peroxide in the system. In an erlenmeyer, 10 mL of the sample was added, followed by 25 mL of water and 10 mL of H_2SO_4 1:5 v/v. The solution was heated until $60 \text{ }^\circ\text{C}$ and titrated with KMnO_4 $4.0 \times 10^{-4} \text{ mol L}^{-1}$. The analysis was carried out in triplicate.

4.9 Total organic carbon (TOC)

The TOC analyses were performed in a Shimadzu OCT-L Analyzer 8 Port-Sampler, which adopts 680°C combustion catalytic oxidation method, the analyzer reach a detection limit of $4 \mu\text{g L}^{-1}$ through coordination with non-dispersive infrared.

Aliquots were taken for each degradation of IBU, NAP and MIX in the time of 0, 20, 40 and 60 min. The volumes were used for analyses of total carbon (TC) and inorganic carbon (IC). The measurements were performed in triplicate and the TOC results were given by the difference among the values obtained for total carbon and inorganic carbon ($\text{TOC} = \text{TC} - \text{IC}$). The Equation 18 presents the % TOC removal calculation.

$$\% \text{TOC} = \frac{\text{TOC}_0 - \text{TOC}_t}{\text{TOC}_0} \cdot 100 \quad \text{Equation 18}$$

where TOC_0 and TOC_t is the total organic carbon in the beginning and the time of the aliquot taken during the degradation, respectively.

4.10 Fluorescence analysis

Fluorescence spectra were acquired on an Agilent Technologies Cary Eclipse fluorescence spectrophotometer with xenon flash lamp. Excitation-emission data arrays were recorded in a 10 mm quartz cell, in the following ranges: excitation, 200 – 260 nm with an increment of 1.5 nm, emission, 267 – 410 nm with an increment of 0.5 nm. The

size of the recorded matrix for each sample was 287×41 . The wavelength scanning speed was 300 nm min^{-1} , excitation and emission slit of 5 nm. The detector voltage was fixed at 600 V.

4.11 PARAFAC model

A calibration curve with 33 mixtures of the standards was built using a mixture design in the range 5.3 to 42.85 mg L^{-1} for IBU and 26 to $212.12 \text{ } \mu\text{g L}^{-1}$ for NAP. The difference in the concentrations of both compounds is due to the difference in the fluorescence of each one. The concentrations were chosen in ranges that could be observed both compounds in the emission spectra. A set of 24 samples were used for calibration, and nine samples were separated for validation. Each mixture had an excitation-emission matrix recorded. The matrixes were organized as three-way data (tensor). Therefore, the tensor $\underline{\mathbf{X}}_{(i,j,k)}$ was obtained with each excitation-emission matrix recorded for the mixture of standards. A simple representation of a tensor is presented in Figure 7. Before the calculations, preprocessing was performed in the data. The Savitzky-Golay algorithm with window 25 and order 2 and baseline was performed. The tensor was unfolded column-wise, and after the preprocessing, the data was refolded. The dimension of the tensor was $33 \times 287 \times 41$ that correspond to samples, emission, and excitation wavelength, respectively.

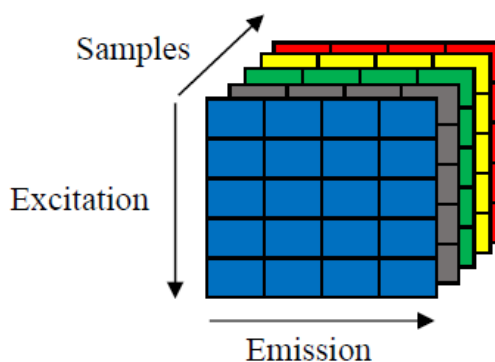


Figure 7: Scheme of a tensor $\underline{\mathbf{X}}$ built with the matrices recorded for each sample.

The number of factors was estimated using the core consistency diagnostic algorithm, CORCONDIA, and residual fit.

Pseudo univariate regression was built using the relative concentrations recovered by the PARAFAC decomposition and the real concentrations of each standard. Also, the spectra profile could be recovered by the method and compared to the standard ones.

4.12 MCR-ALS model

A calibration curve with 33 mixtures of the standards was built, being 24 for calibration and 9 for validation. The tensor $\underline{\mathbf{X}}$ used in the PARAFAC model was unfolded column-wise (Figure 8), and an augmented matrix was obtained. The MCR-ALS was applied to data with a mixture of the standards IBU and NAP in the same concentrations.

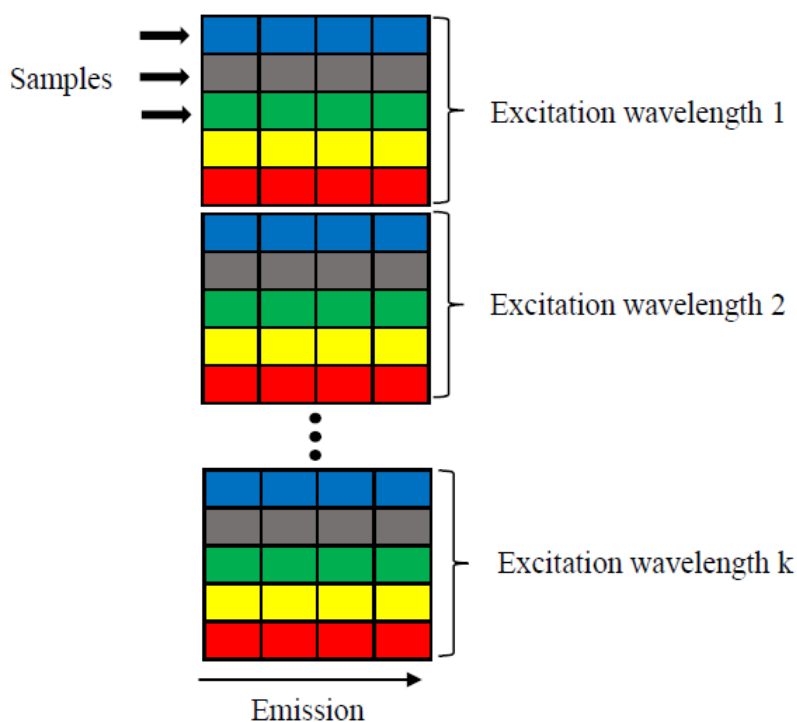


Figure 8: Augmented matrix obtained by unfolding the tensor $\underline{\mathbf{X}}$.

The number of components was estimated by the singular values decomposition (SVD), and an initial estimative of the components spectra was performed using the SIMPLISMA algorithm (WINDIG; STEPHENSON, 1992). The maximum allowed noise from the average spectrum was set to 0.01% for all calculations; non-negativity constraints were applied to the spectrum and concentration.

The pseudo univariate regression was built with the correlation between the relative concentrations recovered by the method MCR-ALS and the known concentrations of the standards in each mixture used in the calibration set.

A single excitation wavelength (242 nm) was fixed, and emission spectra were recorded for each standard. Each emission vector was organized in a matrix $\mathbf{X}_{(ij)}$ (Figure 9) and the method MCR-ALS was performed. 56 standard mixtures were prepared and divided in a calibration set with 39 standards and a validation set with 17 standards. The

concentrations range from 0.042 to 42.85 mg L⁻¹ for IBU and 26 to 212.12 µg L⁻¹ for NAP.

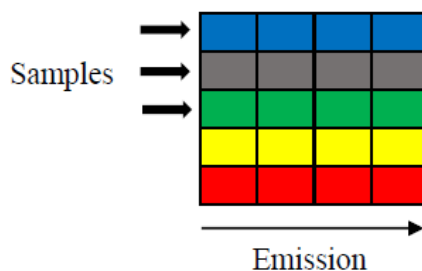


Figure 9: Single matrix recorded at 242 nm excitation wavelength

MCR-ALS was executed with the same parameters and procedure used in the augmented matrix.

4.13 Partial Least Squares Regression (PLSR)

An inverse regression model using PLS was built using the same matrix $X_{(i,j)}$ obtained fixing a single excitation wavelength. The known concentrations of each mixture were used as dependent variable.

A set with 56 mixtures of standards was split into calibration and validation sets using the Kennard-Stone algorithm (KENNARD; STONE, 1969). The number of latent variables was determined by internal validation (cross-validation) where it was applied the random removal of six samples.

4.14 Data treatment

All calculations were performed in Matlab (Matlab R2016a, 9.0, The MathWorks Inc., Natick, USA), PLS-Toolbox 8.2 (Eigenvector Research, Inc. Wenatchee, USA), “N-way Toolbox for MATLAB”(ANDERSSON; BRO, 2000) which is available on the internet at www.models.kvl.dk and MCR-ALS GUI 2.0 which is available on the internet at www.mcrals.info.

4.15 HPLC analyses

Chromatography analyses were conducted to compare the results obtained by the methods PARAFAC, MCR-ALS, and PLS.

A set of mixtures containing IBU and NAP, both in the range 0.10 – 42.0 mg L⁻¹ was used to build a univariate regression with the area referent to the chromatography peak of each compound. The method was developed in a Shimadzu instrument model

20AT Prominence with fluorescence detection. The standards were excited in single wavelength, i.e. (245 nm) and the emission spectrum was recorded in 305 nm.

Separations were carried out in reverse phase with a C18 column Kinetex[®] from Phenomenex, 100 mm × 4.6 mm and 2.6 μm of particle size. The flow rate was maintained in 1 mL min⁻¹, injection volume of 50 μL and oven temperature of 30 °C. The mobile phase consisted of 55 % of formic acid 0.1 mol L⁻¹ and 45 % of acetonitrile.

4.16 Figures of Merit

The quality of the models obtained by the methods MCR-ALS, PARAFAC, PLS, and HPLC were assessed using the root mean square error and correlation coefficient, both described by the equations:

$$RMSE = \sqrt{\frac{\sum_{i=1}^N (y_i - \hat{y}_i)^2}{N}} \quad \text{Equation 19}$$

$$R = \frac{\sum_{i=1}^N (\hat{y}_i - \bar{\hat{y}})(y_i - \bar{y})}{\sqrt{\sum_{i=1}^N (\hat{y}_i - \bar{\hat{y}})^2} \sqrt{\sum_{i=1}^N (y_i - \bar{y})^2}} \quad \text{Equation 20}$$

where y_i and \hat{y}_i are the measured and predicted values, respectively, and N is the number of samples (ROQUE; DIAS; TEÓFILO, 2017). When the samples are present in the calibration set, the error and the correlation coefficient are called RMSEC and R_c , respectively. When the samples are in the validation set, the parameters are RMSEP and R_p .

4.17 Guideline

Table 2 shows an overall of the studies carried out to analyze the data that will be presented in the results and discussion.

Table 2: Overall of the methods and analyses.

Solution	Study	Time	Analysis	Data treatment
MIX	Factorial	4h	COD	DOE
MIX	CCD	4h	COD	DOE
MIX	Models	-	Fluorescence	Multivariate analysis
IBU	Degradation	1h	Fluorescence, HPLC and TOC	Multivariate analysis
NAP	Degradation	1h	Fluorescence, HPLC and TOC	Multivariate analysis
MIX	Degradation	1h	Fluorescence, HPLC and TOC	Multivariate analysis

MIX: mixture of the solutions ibuprofen and naproxen 30 mg L⁻¹ each; IBU: solution of ibuprofen 30 mg L⁻¹; NAP: solution of naproxen 30 mg L⁻¹; DOE: design of experiments; Factorial: 2⁴⁻¹ fractional factorial design with chemical oxygen demand as response (COD); CCD: central composite design with chemical oxygen as response (COD); Models: models built with standard solutions of ibuprofen and naproxen; Multivariate analysis: PARAFAC, MCR-ALS unfolded tensor, MCR-ALS with single excitation matrix (242 nm), PLSR; TOC: total organic carbon

5 RESULTS AND DISCUSSION

5.1 Hydrogen peroxide production

The presence of hydrogen peroxide is one of the most critical parameters in the electron-Fenton process. Electrochemical generation of H_2O_2 in the solution was studied by titration with KMnO_4 to characterize the ability of the system to accumulate H_2O_2 . Studies have shown that *in situ* generation of H_2O_2 in acid medium reduces the high cost related to the consumption of H_2O_2 and simplify the operations during the process (SIRÉS et al., 2014). The reaction that describes this process can be observed in the Equation 6.

In the presence of Fe^{2+} the accumulation could not be performed because the reaction between these species would produce hydroxyl radicals. Therefore, to study the electrogeneration of H_2O_2 , the experiment was done in the absence of Fe^{2+} at pH 3.0 with 5500 mg L^{-1} de Na_2SO_4 , density of current of 45 mA cm^{-2} using BDD anode.

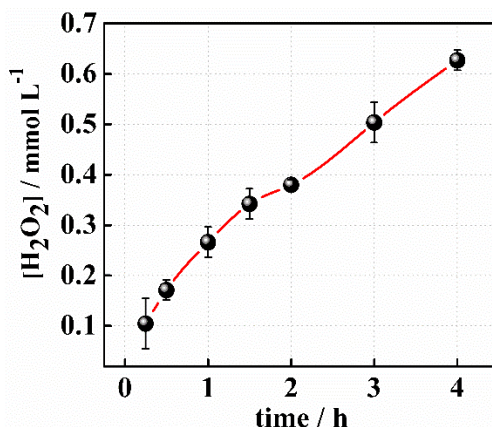


Figure 10: Accumulation of H_2O_2 during the time in the absence of Fe^{2+} .

Hydrogen peroxide reacts with permanganate in the ratio of 5:2 according to the reaction presented in the Equation 21.



The results of each titration assessed during the time are shown in Figure 10. The system was capable of generating from 1.09×10^{-4} to $6.32 \times 10^{-4} \text{ mol L}^{-1}$ of H_2O_2 with relative standard deviation (RSD) between 1 and 6% during four hours. The ability of accumulation of H_2O_2 reveals a functional efficiency of the system to produce this reagent. In this process, H_2O_2 is continuously produced in the solution through the oxygen reduction by two electrons in acid medium (PERALTA-HERNÁNDEZ; GODÍNEZ, 2014). The *in situ* production allows, in the presence of Fe^{2+} , that all the H_2O_2 can be used for the production of hydroxyl radicals by Fenton's reaction.

5.2 Design of Experiments

The efficiency of the mineralization can be associated with parameters such as pH, applied current and presence of a catalyst. Both compounds, IBU and NAP, were degraded during four hours in the conditions defined by experimental design. The parameters that influence the degradation of the compounds and model built were evaluated according to analyses of Pareto chart, response surface plot and ANOVA table.

5.3 2^{4-1} fractional factorial design

The screening experiments using 2^{4-1} fractional factorial design are presented in Table 3 with coded factors in the bracket and the response (%COD) for each experiment run of the mixture.

Table 3: Experimental matrix with decoded, coded factors and %COD response.

Run	<i>j</i>	[Fe ²⁺]	[Na ₂ SO ₄]	Flow	% COD
1	15(-1)	0(-1)	1000(-1)	2.5(-1)	29.6
2	45(+1)	0(-1)	1000(-1)	5.5(+1)	46.9
3	15(-1)	30(+1)	1000(-1)	5.5(+1)	59.9
4	45(+1)	30(+1)	1000(-1)	2.5(-1)	56.7
5	15(-1)	0(-1)	5000(+1)	5.5(+1)	53.0
6	45(+1)	0(-1)	5000(+1)	2.5(-1)	61.2
7	15(-1)	30(+1)	5000(+1)	2.5(-1)	50.5
8	45(+1)	30(+1)	5000(+1)	5.5(+1)	78.2
9	30(0)	15(0)	3000(0)	4.0(0)	59.0
10	30(0)	15(0)	3000(0)	4.0(0)	60.8
11	30(0)	15(0)	3000(0)	4.0(0)	63.2
12	30(0)	15(0)	3000(0)	4.0(0)	60.8

Pareto chart was built in order to identify the main effects for individual parameters and second-order interactions between these parameters. The results can be observed in Figure 11.

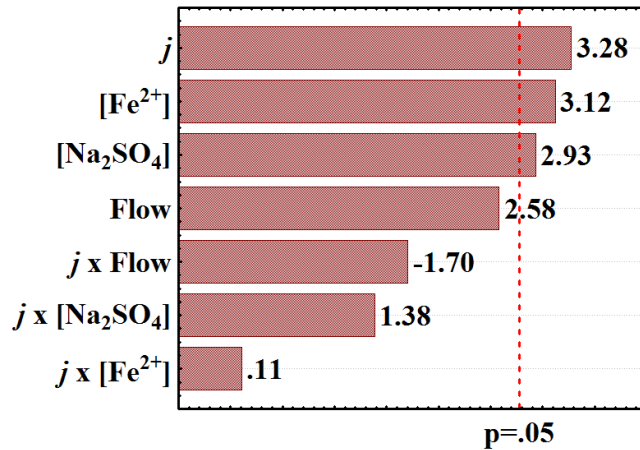


Figure 11: Pareto chart of the standardized effects.

The most important variable that affects electro-Fenton process is the applied current since it is responsible for the rate of generation of hydroxyl radicals (SIRÉS et al., 2014). In this study, density of current, Fe^{2+} , and Na_2SO_4 electrolyte concentration were statistically significant at 5% of significance level by mean square residual error. The density of current was the most important between them. These variable effects were positive, which means that an increase of the parameters causes an increase in the values of % COD removal. The flow rate and second-order interactions were not significant in the levels of the study.

5.4 Central composite design

A CCD with three variables was performed to optimize the variable levels that increase the % COD removal. The variables j , $[Fe^{2+}]$ and $[Na_2SO_4]$ were studied in five levels. The values were based on the levels indicated in the fractional factorial design. A number of 17 experiments were carried out, where 8 are related to the factorial part, 6 for the axial part, and 3 for the central points. As dependent variable for the calculations, it was taken the % COD removal of the mixture in the study. Table 4 shows the experimental matrix with the levels and response for each run.

Table 4: Experimental matrix with decoded and coded variables and response.

Run	<i>j</i>	[Fe ²⁺]	[Na ₂ SO ₄]	% COD
1	35(-1)	20(-1)	4000(-1)	69.8
2	55(+1)	20(-1)	4000(-1)	74.7
3	35(-1)	40(+1)	4000(-1)	70.6
4	55(+1)	40(+1)	4000(-1)	74.3
5	35(-1)	20(-1)	6000(+1)	73.3
6	55(+1)	20(-1)	6000(+1)	75.4
7	35(-1)	40(+1)	6000(+1)	74.5
8	55(+1)	40(+1)	6000(+1)	84.2
9	28.18(- α)	30(0)	5000(0)	77.0
10	61.82(+ α)	30(0)	5000(0)	88.7
11	45(0)	13.18(- α)	5000(0)	74.5
12	45(0)	46.82(+ α)	5000(0)	73.4
13	45(0)	30(0)	3318(- α)	73.9
14	45(0)	30(0)	6682(+ α)	77.0
15	45(0)	30(0)	5000(0)	81.9
16	45(0)	30(0)	5000(0)	79.0
17	45(0)	30(0)	5000(0)	80.3

The model coefficients and their respective errors are presented in Table 5.

Table 5: Regression coefficients and errors of the quadratic model.

Variables	Coefficient	\pm	Error	t (2)	p
mean	80.57	\pm	0.84	95.889	0.0001
<i>j</i>	2.95	\pm	0.39	7.469	0.0175
[Fe ²⁺]	0.62	\pm	0.39	1.574	0.2562
[Na ₂ SO ₄]	1.70	\pm	0.39	4.315	0.0497
<i>j</i> x <i>j</i>	0.28	\pm	0.43	0.645	0.5849
[Fe ²⁺] x [Fe ²⁺]	-2.87	\pm	0.43	6.605	0.0222
[Na ₂ SO ₄]x[Na ₂ SO ₄]	-2.34	\pm	0.43	5.392	0.0327
<i>j</i> x [Fe ²⁺]	0.81	\pm	0.52	1.563	0.2585
<i>j</i> x [Na ₂ SO ₄]	0.41	\pm	0.52	0.787	0.5137
[Fe ²⁺] x [Na ₂ SO ₄]	1.20	\pm	0.52	2.316	0.1465

Table 6 presents the ANOVA of the quadratic regression model. The square regression sum was statistically significant at 5% of significance level, the lack of fit of the model was not significant, which means that the model can predict with confidence.

Table 6: ANOVA of the quadratic model, $\alpha = 0.05$

Analysis of Variance - Quadratic model					
Source	SS	dF	MS	F	p
Regression	329.85	9	36.65	4.80*	0.0254
Residual	53.50	7	7.64		
Lack of fit	49.25	5	9.85	4.63	0.1871
Pure Error	4.25	2	2.13		
Total	383.35	16			
% Explained variance				86.04	
% Max. explained variance				98.89	

*Significant ($p < \alpha$)

The model equation was recalculated using only the significant variables. The adjusted Equation 22 represents the fitted model.

$$\% \text{ COD} = \underset{\pm 0.61}{80.93} + \underset{\pm 0.41}{2.95} j + \underset{\pm 0.41}{1.70} [\text{Na}_2\text{SO}_4] - \underset{\pm 0.69}{2.95} [\text{Fe}^{2+}]^2 - \underset{\pm 0.69}{2.42} [\text{Na}_2\text{SO}_4]^2$$

Equation (22)

where, j , $[\text{Fe}^{2+}]$ and $[\text{Na}_2\text{SO}_4]$ are the independent variables coded values.

The significant coefficients are shown in bold in Table 5. They are related to those variables that were the most important to cause an increase in the %COD removal. The %COD removal is mainly affected linearly by the applied density of current and the concentration of Na_2SO_4 . Also, it is affected by the squared terms of iron(II) and Na_2SO_4 concentration, the values of the coefficients shows that a linear increase in the coded values of density of current and the concentration of Na_2SO_4 will cause an increase in the %COD removal, followed by a quadratic decrease in the coded values of iron(II) and Na_2SO_4 concentration.

The concentration of iron(II) has a huge importance in electron-Fenton process because it acts as a catalyst in the solution (SIRÉS et al., 2014), high concentration of this reagent can cause parallel reactions and decrease the production of hydroxyl radical, on the contrary, low concentrations will not be able to catalyze the reaction (SIRÉS et al., 2014; SKOUMAL et al., 2009). Studies related to the concentration of Fe^{2+} on the degradation of synthetic dyes using electron-Fenton process showed that values between 28 mg L^{-1} mM and 56 mg L^{-1} of Fe^{2+} gave 89% - 93% in the % COD removal (PANIZZA; CERISOLA, 2008).

Ibuprofen was degraded using non-thermal dielectric barrier discharged combined with Fenton's reaction using 10 mg L^{-1} of Fe^{2+} . The results showed that such concentration of Fe^{2+} did not have significant improvement in the degradation of the compound (HIKMAT et al., 2017). Madhavan and Skoumal studied different processes

using $20 \text{ mg L}^{-1} \text{ Fe}^{3+}$ and $30 \text{ mg L}^{-1} \text{ Fe}^{2+}$, respectively, in the degradation of ibuprofen and could observe an enhancement in the degradation of the compound (MADHAVAN; GRIESER; ASHOKKUMAR, 2010; SKOUMAL et al., 2009). Fenton' reaction was used with 30 mg L^{-1} of Fe^{2+} to degrade naproxen; the results showed almost total mineralization of the molecule (91 % of TOC removal) (CORIA et al., 2016).

In this work, the linear concentration of iron (II) was not significant in the response. Skoumal has described that an increase in the degradation rate can be observed when the initial catalyst rises from 5.6 to 30 mg L^{-1} (SKOUMAL et al., 2009). The literature shows a vast number of papers that use concentration around 30 mg L^{-1} of Fe^{2+} . Here, it was fixed the decoded value at 30 mg L^{-1} (central point) in order to build a surface response plot.

Fixing the concentration of Fe^{2+} , a response surface as a function of the applied density of current and Na_2SO_4 concentration was built.

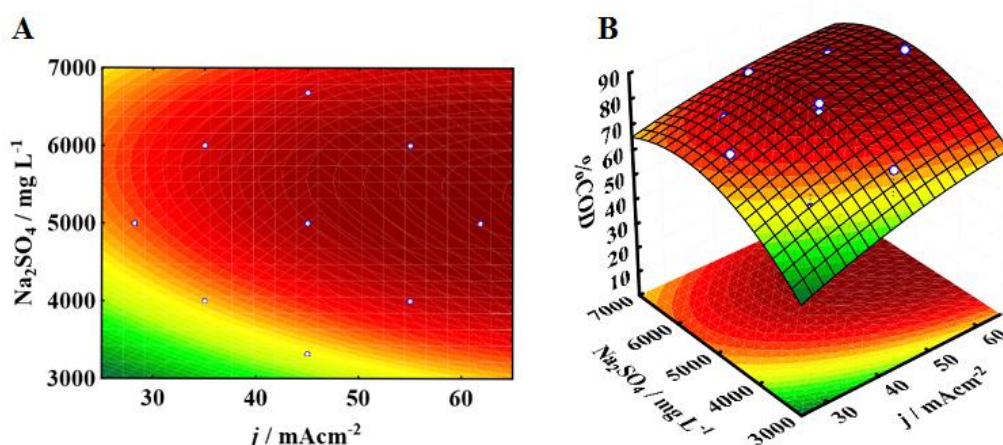


Figure 12: Contour plot and response surface plot of the %COD removal as a function of Na_2SO_4 concentration and applied density of current, iron (II) concentration fixed at 30 mg L^{-1} .

Both plots presented in Figure 12 shows how the %COD removal is influenced by the factors in the study. From Figure 12, it is possible to take the estimative value of density of current that should be applied in the system that will give the best rate of degradation; the same procedure can be done to the concentration of Na_2SO_4 . By analyzing these plots, it can be concluded that an increase of both parameters will cause an increase in the %COD removal keeping Fe^{2+} fixed in 30 mg L^{-1} . Thus, the factors were optimized accordingly; the best conditions to execute the degradation of IBU and NAP employing the levels studied are applying 60 mA cm^{-2} of density of current, 30 mg L^{-1} of Fe^{2+} and 5500 mg L^{-1} of Na_2SO_4 .

Some methods in the literature describe conditions with higher values for density of current, Fe^{2+} concentration and electrolyte concentration in the degradation of different types of compounds (BRILLAS et al., 2004; DOMÍNGUEZ et al., 2010; PANIZZA; CERISOLA, 2008). Ibuprofen was degraded in a system in the presence of 30 mg L^{-1} Fe^{2+} at 100 mA cm^{-2} for 360 minutes, 81% TOC removal was achieved (SKOUMAL et al., 2009). 40 mg L^{-1} of naproxen was degraded using electro-Fenton and Photoelectron-Fenton process with 50 mA cm^{-2} , 30 mg L^{-1} of Fe^{2+} during 4h achieving 85% of TOC removal (CORIA et al., 2016). Therefore, the optimized method is attractive compared to some methods found in the literature, once it requires less time of degradation.

The energetic efficiency achieved for the optimized method was 150 kW h m^{-3} . Even though the energetic efficiency seems to be high, when it is compared to works in the literature, the advantage is related to the time of degradation, the most published works use degradation time around 4 to 6h. The method proposed here could achieve excellent results in just one hour as it will be presented.

5.5 Degradation of the compounds

The optimized method was employed in the degradation of 30 mg L^{-1} of IBU, 30 mg L^{-1} of NAP and a mixture of both compounds in the same concentrations. Aliquots were taken over the time and analyzed through TOC and fluorescence spectroscopy. TOC was applied to verify the mineralization efficiency of degradation. TOC was used in this step due to the low concentration that can be achieved after the degradation; the technique can determine low concentrations due to the low detection limits.

The collected fluorescence data were analyzed using chemometrics methods such as MCR-ALS, PARAFAC and PLSR. HPLC was also applied to validate and to confirm the accuracy of the chemometric method.

5.6 Fluorescence spectra

5.6.1 Regression methods from chemometric methods and HPLC

IBU and NAP have their emission wavelength in approximately 290 and 350 nm, respectively. Initially, fluorescence data was acquired from standard mixtures of IBU and NAP to build models with each chemometric method. Table 7 shows the calibration parameters for the models built using a mixture of standards.

Excellent linearity was achieved by the models, which demonstrates the high accuracy of the methods. The best multivariate model was obtained using a single matrix

with fixed wavelength by the MCR-ALS method, Figure 13 shows the correlation between the measured and predicted values by the models for both compounds.

Table 7: Calibration parameters obtained for the methods PARAFAC, MCR-ALS and HPLC using standards.

Compound	Parameters	PARAFAC	MCR-ALS*	MCR-ALS**	HPLC	PLS
IBU	Range / mg L ⁻¹	5.30 - 42.85	5.30 - 42.85	0.042 - 42.85	0.10 - 42.0	5.30 - 42.85
	Rc	0.9956	0.9985	0.9989	0.9996	0.979
	RMSEC / mg L ⁻¹	1.085	0.6446	0.6599	0.1973	0.6627
	RMSEP / mg L ⁻¹	1.067	0.6919	0.6473	0.3941	0.5035
	Rp	0.9971	0.9995	0.9984	0.9995	0.9997
	% EV	99.12	99.70	99.78	99.92	99.21
NAP	Range / mg L ⁻¹	0.026 - 0.212	0.026 - 0.212	0.026 - 0.212	0.10 - 42.0	0.026 - 0.212
	Rc	0.9558	0.9548	0.9986	0.9998	0.989
	RMSEC / mg L ⁻¹	0.0170	0.0173	0.0037	0.1994	2.6815
	RMSEP / mg L ⁻¹	0.0171	0.0166	0.0026	0.1773	1,888
	Rp	0.9637	0.9667	0.9994	0.9999	0.9996
	% EV	91.35	91.16	99.72	99.96	99.49

*Model built with unfolded tensor.

**Model built with a single matrix $\lambda_{exc} = 242$ nm.

The results achieved from the tensor was not so impressive for NAP correlations, even though IBU had excellent correlations. This fact can be associated with quenching phenomenon. The fluorescence phenomenon is related to the concentration of the sample, which can affect the fluorescence intensity of the fluorophores present in the solution directly. Quenching is an important factor that might be present in the fluorescence spectra (TREVISAN, 2003). Because of the difference between the sensitivity of the molecules in this study, quenching was detected at some point in low levels. The high fluorescence sensitivity of NAP compared to the IBU could have caused a decrease in the emission spectra of the NAP which brought a slight decrease in the linearity. These results can be observed in the models for the tensor data using PARAFAC and MCR-ALS. The quenching related to self-absorption can occur when there is overlapping of excitation and/or emission bands (TREVISAN, 2003), in the case of NAP and IBU, overlapping can be observed in the excitation wavelength of both molecules. The interaction between IBU and NAP cause a loss in the fluorescence emission of the NAP because IBU or solvent molecules might absorb part of the NAP emission that should reach the detector and thereat there was not possible to achieve a good correlation for NAP using the methods PARAFAC and MCR-ALS using the tensor and unfolded tensor data.

The model using the PLS method was good, however; for prediction of the samples values, the model could not predict it with accuracy. The reason is that for the samples, there were present some components which were not included in the building of the

model. PLS is able to predict in the presence of interferences, but the interferences must be in the calibration set. The byproducts generated during the degradation were not present in the calibration of the PLS model. Therefore, the results for prediction of samples were not good and were not considered.

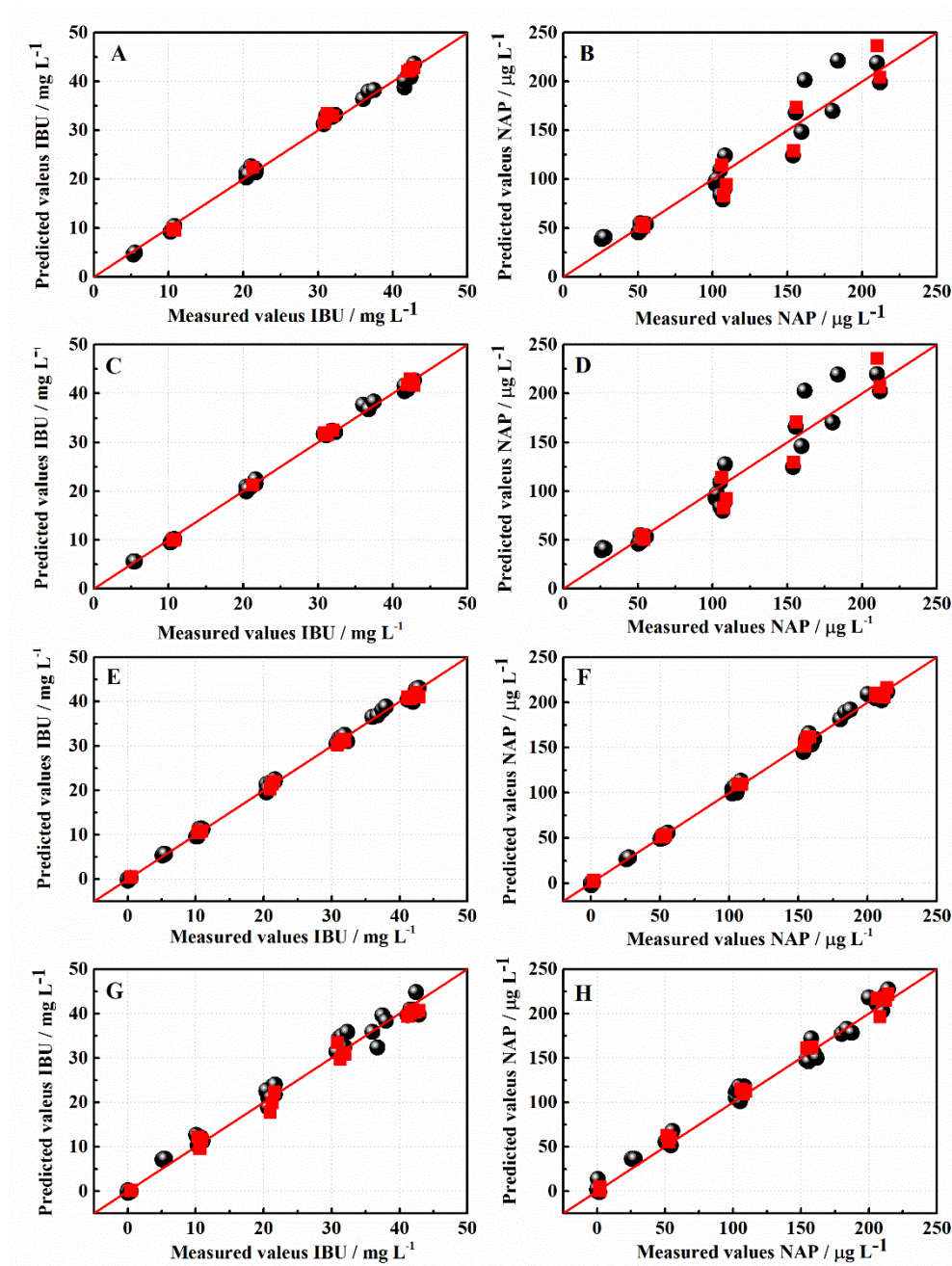


Figure 13: Correlation between the measured and predicted values by the models. PARAFAC model IBU (A) and NAP (B), MCR-ALS model unfolded tensor IBU (C) and NAP (D), MCR-ALS $\lambda=242$ nm. IBU (F) and NAP (E), PLSR model IBU (G) and NAP (H). Calibration set (●) and validation set (■).

On the other hand, an excellent correlation was reached between the measured and predicted values using the single matrix taken from the tensor data applying MCR-ALS.

In the fixed excitation wavelength (242 nm), quenching was not observed. In the case of the tensor, a range of excitation wavelength was chosen to be scanned; the quenching phenomenon might have been significant in some of the excitation wavelengths during the scanning, which causes more interactions between the compounds or solvent in the excited ground (BOWEN, 1947; TREVISAN, 2003). When only one excitation was fixed, quenching might not have occurred at this value, which might explain the excellent correlation between the results for MCR-ALS using a single matrix at 242 nm.

5.7 Application of the best model

The best model was achieved by MCR-ALS method using the single matrix with a fixed excitation wavelength (242 nm). The results of this method will be presented in the next pages for the degradation of IBU, NAP, and MIX. The norm of the fluorescence spectra for each degradation was calculated using the Equation $\| \text{signal} \| = \sqrt{x^t \cdot x}$, where x is a vector of the fluorescence spectra.

5.7.1 Ibuprofen results

Figure 14 displays the norm of the fluorescence intensity for the aliquots taken from the degradation of IBU. As it can be seen, there is a decrease in the signal of the compound along the time which indicates that the fluorescence of the molecule is decreasing. It is possible to note an increase of the norm of the signal between 10 and 20 minutes; it can be associated to the formation of molecules that have a quantum yield higher than the original molecule (IBU). The formation of byproducts over the degradation time was expected since the hydroxyl radical is not selective and can attack the molecules in different ways. The norm shows that the kinetics of the reaction is quick, in 5 minutes the fluorescence signal decrease significantly. Even though the norm of the signal has increased at that time; the norm signal decreased after 20 minutes, which suggest the formation and elimination of these byproducts with high quantum yield.

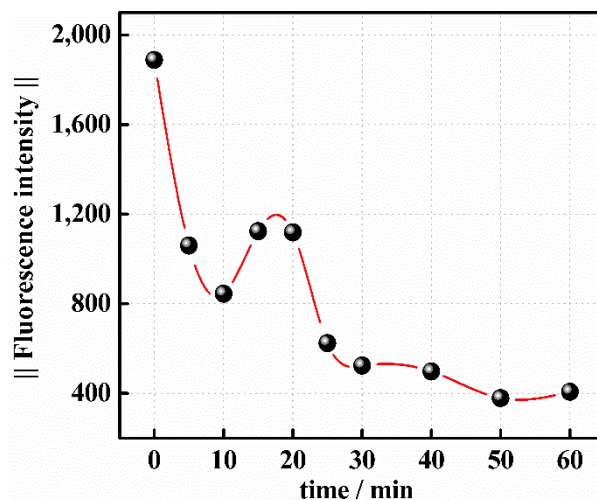


Figure 14: Norm of the fluorescence intensity over the time.

The MCR-ALS was applied to the matrix in order to identify the pure spectra and relative concentrations of the compounds present in the data matrix. Figure 15 shows the results obtained for IBU degradation.

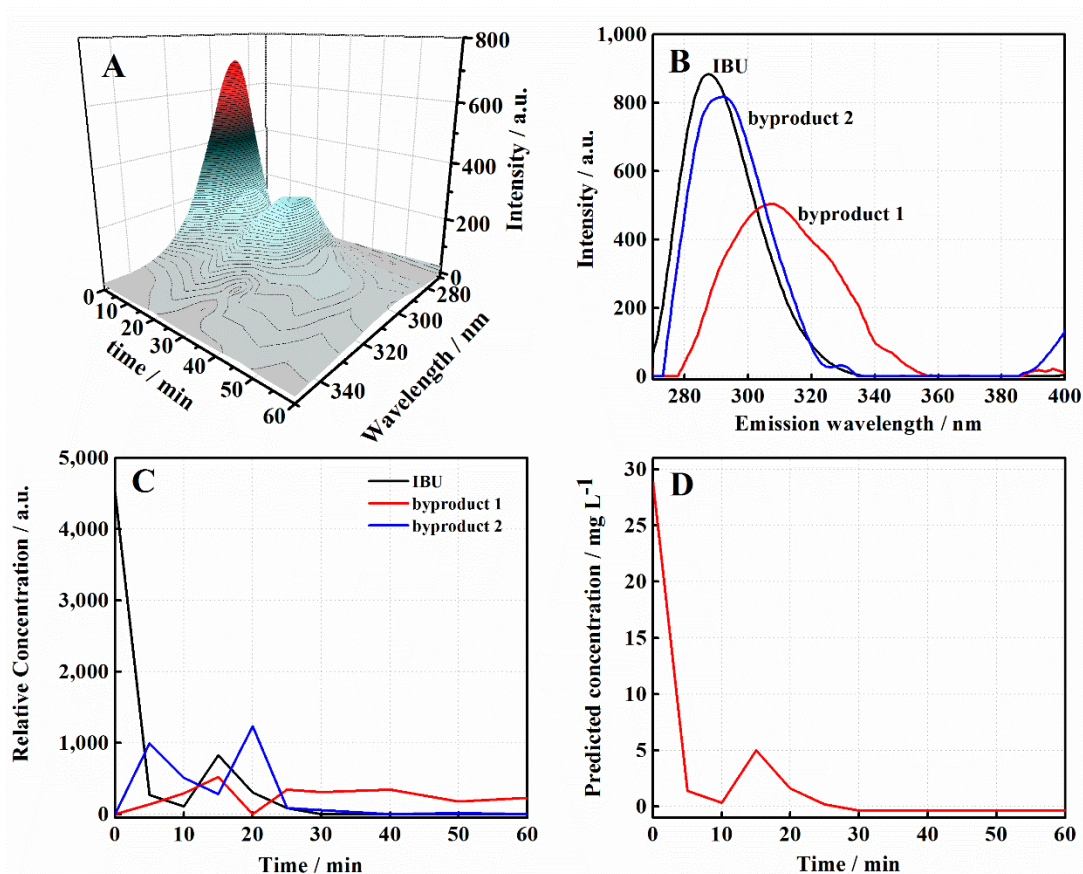


Figure 15: Resolution of MCR-ALS for degradation of IBU. (A) Surface 3D of the fluorescence spectra over the time, (B) Recovered pure spectra of the estimated compounds. (C) Relative concentrations of the estimated compound. (D) Concentration predicted by the model.

The number of components estimated by the algorithm SVD was three, which are related to the presence of the target compound (IBU) and two byproducts that were generated during the degradation. The statistical parameters for the resolution using the method were %lack of fit (LOF), and % explained variance (%EV), which were 4.19% and 99.82%, respectively. Those parameters allow assessing the dissimilarity among the experimental data matrix and the data modeled by MCR-ALS. Therefore, the resolution presented an excellent spectral prediction with small %LOF and excellent %EV. The concentrations of IBU could be assessed using the relative concentrations recovered by the method, and the model built. Figure 15 (D) present the IBU concentrations predicted by the model, IBU concentration decreased over the time, which means that the fluorescence of the molecule decreased significantly and was degraded efficiently. The results in Figure 15 (C) that show increasing and decreasing in the relative concentrations can be explained by the rank deficient of the matrix, which recognizes different spectra profile that are very similar as just one spectrum.

5.7.2 Naproxen results

The norm of the fluorescence spectra was calculated and are presented in Figure 16. The fluorescence signal of the compound decreased expressively. The slightly increase that can be observed at some points in Figure 16 can be associated to the presence of byproducts that fluoresce and contribute to the fluorescence signal having a quantum yield higher than other molecules formed over the degradation. The kinetics of the reaction is very similar to IBU, the signal decrease quickly over the time.

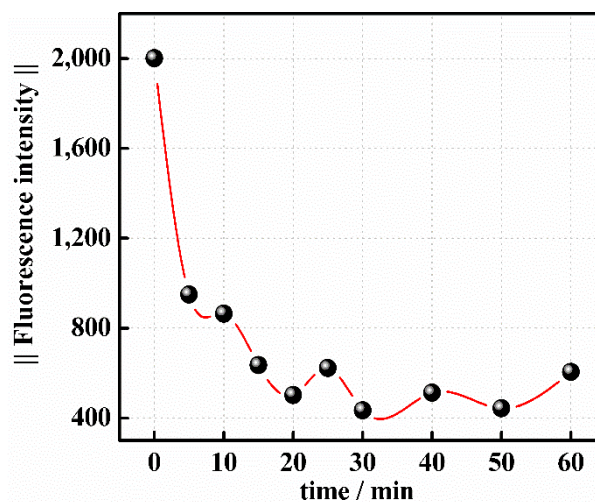


Figure 16: Norm of the fluorescence intensity during the time.

MCR-ALS was carried out to degradation data of NAP; the results are presented in Figure 17. The number of components estimated by the SVD algorithm was three, the resolution presented good values of %LOF and %EV, which are 6.88% and 99.53%, respectively

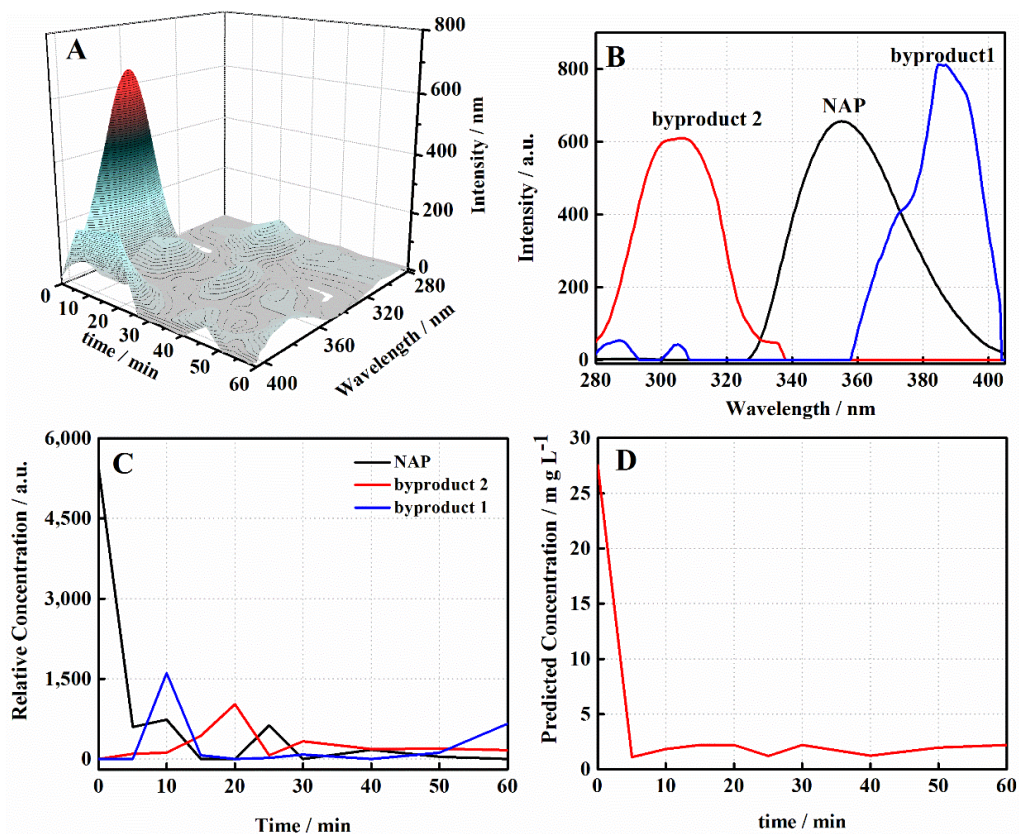


Figure 17: Resolution of MCR-ALS for degradation of NAP. (A) Surface 3D of the fluorescence spectra through the time, (B) Recovered pure spectra of the estimated compounds. (C) Relative concentrations of the estimated compound. (D) Concentration predicted by the model.

The method was able to recover the pure spectra of the NAP and two byproducts generated during the degradation. The model built using the method was used to predict the concentrations of NAP during the time, the results show that the degradation of NAP was performed with effectiveness and the method MCR-ALS is very powerful to extract the relevant information of the data mathematically. The rank deficient was observed as well as in the IBU degradation, the number of significant contributions to the data variance is lower than the number of chemical components.

5.7.3 Mixture results

The degradation of the mixture was carried out, and the norm of the fluorescence spectra is presented in Figure 18. It is possible to notice that there is a decrease in the

signal. However, the decrease cannot be directly associated with the degradation of the compounds IBU and NAP. Along the process, the generation of byproducts can contribute to the total signal. Therefore, the high increase of the norm in 40 min can be associated with species with high quantum yield. The kinetics of the reaction is lower than for the degradation of the individual compounds; it can be related to the concentration of the mixture, which is twice higher than for the individual compounds.

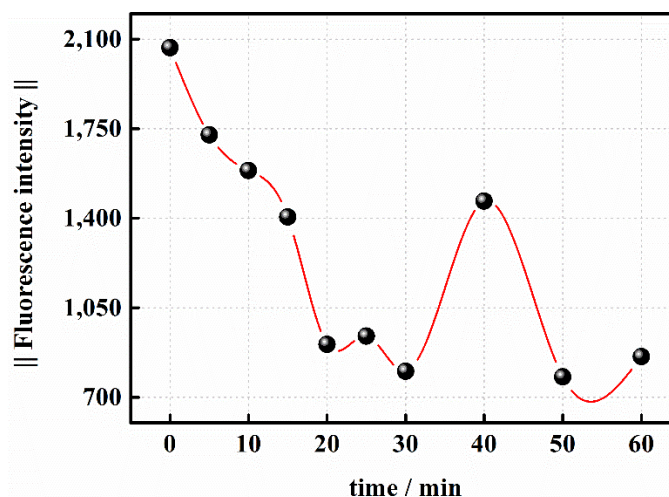


Figure 18: Norm of the fluorescence spectra for the mixture.

The method MCR-ALS was performed to identify the possible products generated from the degradation of the mixture. Figure 19 displays the results obtained by the method.

The number of components present in the experimental data was determined as five using the SVD algorithm. They are related to the NAP, IBU and three byproducts generated during the degradation. The spectral recovered presented 3.56 % of LOF and 99.87% of explained variance, which demonstrates a high capability of the method to solve the problem of overlapping between the spectra of the compounds. The concentration of NAP and IBU was determined using the built models for each compound, and the results showed reasonable rate for the degradation of both compounds, even in the mixture. The rank deficient was observed for the mixture just as for the degradation of individual compounds.

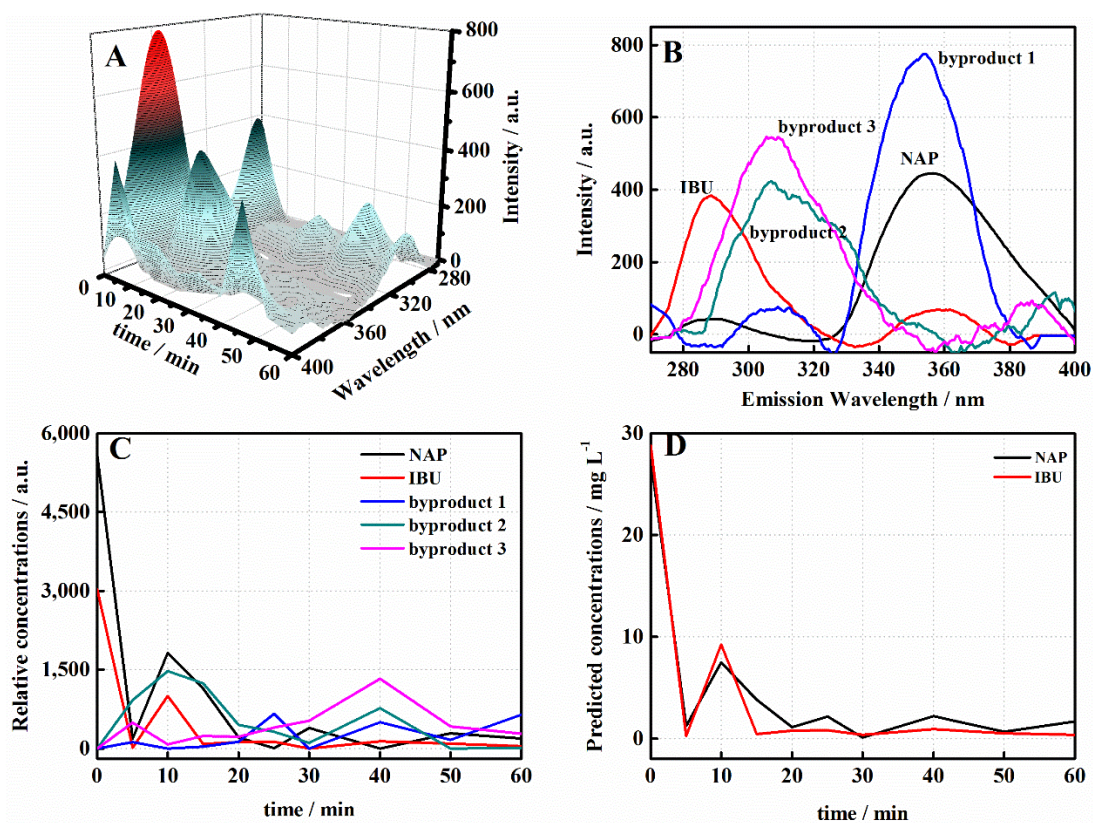


Figure 19: Resolution of MCR-ALS for degradation of MIX. (A) Surface of the fluorescence spectra through the time, (B) Recovered pure spectra of the estimated compounds. (C) Relative concentrations of the estimated compound. (D) Concentrations predicted by the model.

The fluorescence technique is very selective and excellent to monitor the degradation of molecules that fluoresce. Usually, when part of a molecule that is responsible for the toxicity is broken, the fluorescence is eliminated or minimized. This happens because, in most of the cases, the rigid bonds are responsible for the fluorescence phenomenon. Also, these bonds are the part of the molecules that propitiate the high toxicity, such as molecules with aromatic rings. In this work, the electrodegradation process proposed led to the rapid elimination of the activity of the molecules IBU and NAP in a small period. It is possible to notice that some byproducts were generated during the process, which would be a concern; however, the relative concentrations recovered by the method MCR-ALS suggest that the fluorescence of these compounds is also minimized. Therefore, after the degradation process, the solution is probably less toxic than the original one because the aromatic rings of the compounds were eliminated.

5.8 HPLC results

HPLC analyses were conducted to compare the results obtained by the method MCR-ALS. The chromatograms for the degradation of IBU, NAP, and MIX are presented in Figure 20.

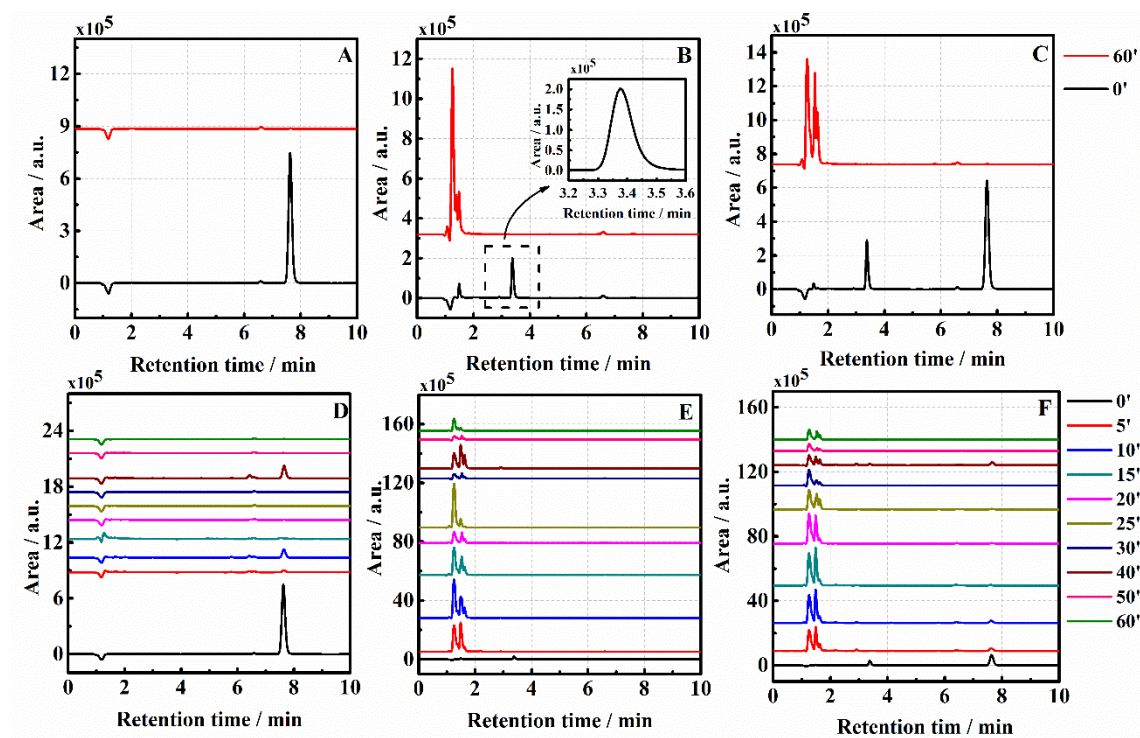


Figure 20: Chromatography runs for aliquots taken from IBU (A and D), NAP (B and E) and MIX (C and F). Above are shown just the first and final aliquot, below there are all the aliquots taken from each degradation.

The chromatography method developed for the analyses showed that the retention time for IBU is 7.65 minutes and for NAP, 3.33 minutes using the studied conditions. As it can be seen, in the chromatogram of the aliquots above, both compounds could be identified in their retention time and a decreasing in the peak along the time is perceptible. The chromatogram also displays some different peaks before 2 minutes that might be associated with the byproducts generated during the degradation.

The concentration of each compound was estimated using the HPLC model and compared to the others obtained by MCR-ALS. The results are presented in Figure 21.

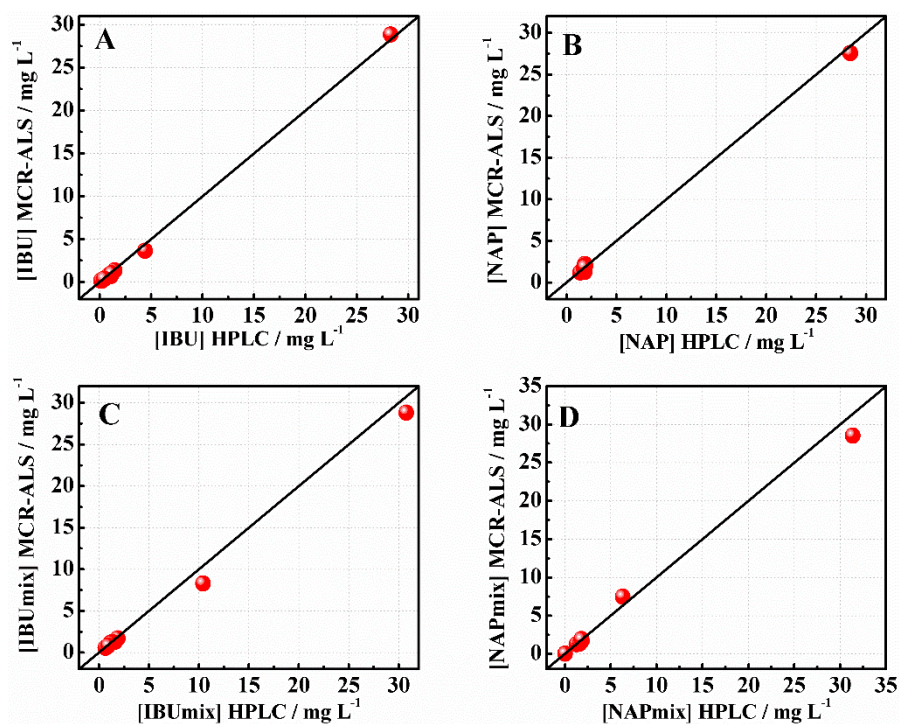


Figure 21: Measured versus Predicted values of IBU and NAP concentrations estimated by MCR-ALS and HPLC. IBU degradation (A), NAP degradation (B) and MIX degradation (C and D).

Correlations of 0.9973 and higher were obtained between the values of concentrations predicted by the method MCR-ALS and the HPLC, which demonstrate the ability of the chemometric model in the determination of the compounds compared to routine analysis. The HPLC results show that the method using electron-Fenton process with BDD as an anode with fluorescence technique detection was very efficient to degrade the compounds, the decreasing in the area of chromatogram peaks reveal 97% and 94% of removal of IBU and NAP, respectively.

5.9 TOC results

Analyses of TOC was performed to each degradation over the time. The TOC analyses were important to evaluate the rate of mineralization of the compounds. From the fluorescence spectra, we can suggest the elimination of the toxicity of the molecules based on the fluorescence decrease. TOC permits to evaluate the removal of organic matter in the solution. The results obtained for %TOC removal are presented in Figure 22.

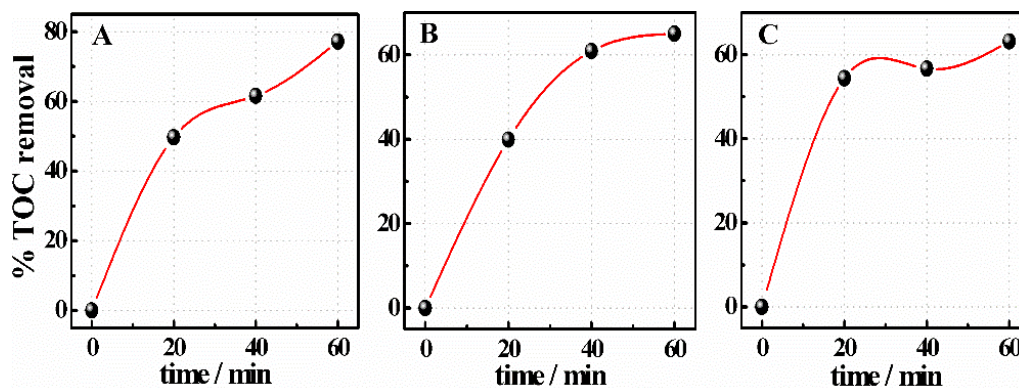


Figure 22: Total carbon organic removal, values are given in percentage. IBU (left side), NAP (middle) and MIX (right side).

The results show a good increase in the percentage removal of total organic carbon for the degradation samples, which can suggest that the compounds were mineralized efficiently by the process. %TOC removal was about 77%, 65% and 63% for IBU, NAP, and MIX, respectively. As we could see, the method electro-Fenton using BDD anode was very efficient in the degradation of the compounds.

The chemometric method used in this work take less time, it is environmentally friendly, since the use of reagents is minimized, fast and straightforward. Thus, it shows to be a powerful tool in the analyses of pharmaceutical compounds, such as IBU and NAP.

6 CONCLUSIONS

The CCD fitted model was adequately applied to choose the best variable levels that optimized the electro-Fenton process. The main factors in the electro-Fenton process using BDD were the concentration of Na_2SO_4 and the current density. The electrodegradation of IBU, NAP, and MIX was efficiently performed using the optimized system. The monitoring of the degradations was adequately carried out using fluorescence spectra, HPLC and TOC. Models PARAFAC, MCR-ALS, and PLSR were built to analyze the fluorescence spectra. The best model was using a fixed excitation wavelength with the MCR-ALS method. The model MCR-ALS fitted was able to recover the pure spectra profile of the IBU, NAP and some byproducts. Using fluorescence spectra and MCR-ALS, IBU and NAP concentration were determined during the degradation and in the presence of unknown interferers. These results were compared to HPLC analyses, and high correlations were obtained. The breaking of the aromatic rings detected by the rapid decrease in fluorescence during the process suggests a decrease in the toxicity of the solutions. The optimized process using BDD provided an excellent ratio in the degradation of the studied compounds showing excellent values of %TOC removal in just one hour. Therefore, the electro-Fenton degradation of IBU and NAP was efficient and can be monitored using fluorescence spectroscopy and MCR-ALS. The analytical monitoring method presented proved to be simple, fast, environmentally friendly and an excellent alternative to routine HPLC analyses.

7 REFERENCES

ABD, M. et al. Spectrochimica Acta Part A: Molecular and Biomolecular Spectroscopy Two and three way spectrophotometric-assisted multivariate determination of linezolid in the presence of its alkaline and oxidative degradation products and application to pharmaceutical. v. 128, p. 231–242, 2014.

ACAR, E.; YENER, B. Unsupervised Multiway Data Analysis: A Literature Survey. **IEEE Transactions on Knowledge and Data Engineering**, v. 21, n. 1, p. 6–20, jan. 2009.

ANDERSEN, C. M.; BRO, R. Practical aspects of PARAFAC modeling of fluorescence excitation-emission data. **Journal of Chemometrics**, v. 17, n. 4, p. 200–215, 2003.

ANDERSSON, C. A.; BRO, R. The N-way Toolbox for MATLAB. **Chemometrics and Intelligent Laboratory Systems**, v. 52, n. 1, p. 1–4, 2000.

ANDREOZZI, R. Advanced oxidation processes (AOP) for water purification and recovery. **Catalysis Today**, v. 53, n. 1, p. 51–59, 1999.

BAHRAM, M. et al. Handling of Rayleigh and Raman scatter for PARAFAC modeling of fluorescence data using interpolation. n. January, p. 99–105, 2007.

BARBUSIŃSKI, K. Controversy Over Fenton Mechanism. **Ecol. Chem. Eng. S.**, v. 16, n. 3, p. 347–358, 2009.

BOGER, B. et al. Micropoluentes emergentes de origem farmacêutica em matrizes aquosas do Brasil: uma revisão sistemática Pharmaceutical micropollutants in brazilian aqueous samples: A systematic review. **Ciência e Natura**, v. 37, p. 725–739, 2015.

BOWEN, E. J. Fluorescence and fluorescence quenching. **Quarterly Reviews, Chemical Society**, v. 1, n. 1, p. 1, 1947.

BRILLAS, E. et al. Electrochemical destruction of chlorophenoxy herbicides by anodic oxidation and electro-Fenton using a boron-doped diamond electrode. **Electrochimica Acta**, v. 49, p. 4487–4496, 2004.

BRILLAS, E.; SIRÉS, I.; OTURAN, M. A. Electro-Fenton Process and Related Electrochemical Technologies Based on Fenton's Reaction Chemistry. **Chemical Reviews**, v. 109, n. 12, p. 6570–6631, 9 dez. 2009.

BRO, R. PARAFAC . Tutorial and applications. v. 38, p. 149–171, 1997.

CAÑAS, A.; RICHTER, P.; ESCANDAR, G. M. Chemometrics-assisted excitation-emission fluorescence spectroscopy on nylon-attached rotating disks. Simultaneous determination of polycyclic aromatic hydrocarbons in the presence of

interferences. **Analytica Chimica Acta**, v. 852, p. 105–111, 2014.

CASTENSSON, S. et al. A method to include the environmental hazard in drug prescribing. **Pharm World Sci**, v. 31, p. 24–31, 2009.

CHRISTENSEN, F. M. Pharmaceuticals in the Environment—A Human Risk? **Regulatory Toxicology and Pharmacology**, v. 28, n. 3, p. 212–221, dez. 1998.

CORIA, G. et al. Influence of the anode material on the degradation of naproxen by Fenton-based electrochemical processes. **Chemical Engineering Journal**, v. 304, p. 817–825, nov. 2016.

CRUZ-RIZO, A. et al. Application of electro-Fenton/BDD process for treating tannery wastewaters with industrial dyes. **Separation and Purification Technology**, v. 172, p. 296–302, 2017.

DAUGHTON, C. G. Non-regulated water contaminants: Emerging research. **Environmental Impact Assessment Review**, v. 24, n. 7–8, p. 711–732, 2004.

DE JONG, S. SIMPLS: An alternative approach to partial least squares regression. **Chemometrics and Intelligent Laboratory Systems**, v. 18, n. 3, p. 251–263, mar. 1993.

DE JUAN, A.; JAUMOT, J.; TAULER, R. Multivariate Curve Resolution (MCR). Solving the mixture analysis problem. **Anal. Methods**, v. 6, n. 14, p. 4964–4976, 2014.

DOMÍNGUEZ, J. R. et al. Anodic oxidation of ketoprofen on boron-doped diamond (BDD) electrodes. Role of operative parameters. **Chemical Engineering Journal**, v. 162, n. 3, p. 1012–1018, 1 set. 2010.

ESCANDAR, G. M. et al. Second- and higher-order data generation and calibration: A tutorial. **Analytica Chimica Acta**, v. 806, p. 8–26, 2014.

FENG, L. et al. Removal of residual anti-inflammatory and analgesic pharmaceuticals from aqueous systems by electrochemical advanced oxidation processes. A review. **Chemical Engineering Journal**, v. 228, p. 944–964, 2013.

FENG, L. et al. Degradation of anti-inflammatory drug ketoprofen by electro-oxidation: Comparison of electro-Fenton and anodic oxidation processes. **Environmental Science and Pollution Research**, v. 21, n. 14, p. 8406–8416, 2014.

FERREIRA, M. M. C. et al. Quimiometria I: calibração multivariada, um tutorial. **Química Nova**, v. 22, n. 5, p. 724–731, set. 1999.

GENTILI, A. Determination of non-steroidal anti-inflammatory drugs in environmental samples by chromatographic and electrophoretic techniques. **Analytical and Bioanalytical Chemistry**, v. 387, n. 4, p. 1185–1202, 6 fev. 2007.

HARSHMAN, R. A.; LUNDY, M. E. PARAFAC: Parallel factor analysis.

Computational Statistics & Data Analysis, v. 18, n. 1, p. 39–72, ago. 1994.

HEBERER, T. Occurrence, fate, and removal of pharmaceutical residues in the aquatic environment: a review of recent research data. **Toxicology Letters**, v. 131, n. 1–2, p. 5–17, maio 2002.

HIKMAT, K. et al. Degradation of pharmaceutical diclofenac and ibuprofen in aqueous solution, a direct comparison of ozonation, photocatalysis, and non-thermal plasma. **Chemical Engineering Journal**, v. 313, p. 1033–1041, 2017.

ISIDORI, M. et al. Ecotoxicity of naproxen and its phototransformation products. **Science of The Total Environment**, v. 348, n. 1–3, p. 93–101, set. 2005.

JAUMOT, J.; DE JUAN, A.; TAULER, R. MCR-ALS GUI 2.0: New features and applications. **Chemometrics and Intelligent Laboratory Systems**, v. 140, p. 1–12, 2015.

KANAKARAJU, D. et al. TiO₂ photocatalysis of naproxen: Effect of the water matrix, anions and diclofenac on degradation rates. **Chemosphere**, v. 139, p. 579–588, nov. 2015.

KENNARD, R. W.; STONE, L. A. Computer Aided Design of Experiments. **Technometrics**, v. 11, n. 1, p. 137, fev. 1969.

KOWALSKI, B. R. Chemometrics. **Analytical Chemistry**, v. 52, n. 5, p. 112–122, abr. 1980.

KÜ, K. The presence of pharmaceuticals in the environment due to human use – present knowledge and future challenges. **Journal of Environmental Management**, v. 90, p. 2354–2366, 2009a.

KÜ, K. The presence of pharmaceuticals in the environment due to human use – present knowledge and future challenges. **Journal of Environmental Management**, v. 90, p. 2354–2366, 2009b.

LINDGREN, F.; GELADI, P.; WOLD, S. The kernel algorithm for PLS. **Journal of Chemometrics**, v. 7, n. 1, p. 45–59, jan. 1993.

LUNDSTEDT, T. et al. Experimental design and optimization. **Chemometrics and Intelligent Laboratory Systems**, v. 42, n. 1–2, p. 3–40, 1998.

MADHAVAN, J.; GRIESER, F.; ASHOKKUMAR, M. Combined advanced oxidation processes for the synergistic degradation of ibuprofen in aqueous environments. **Journal of Hazardous Materials**, v. 178, n. 1–3, p. 202–208, 2010.

MARÇO, P. H. et al. Multivariate Curve Resolution With Alternating Least Squares: Description, Operation and Applications. **Química Nova**, v. 37, n. 9, p. 1525–

1532, 2014.

MARSELLI, B. et al. Electrogenation of Hydroxyl Radicals on Boron-Doped Diamond Electrodes. **Journal of The Electrochemical Society**, v. 150, n. 3, p. D79, 2003.

MARTINS, J. P. A.; TEÓFILO, R. F.; FERREIRA, M. M. C. Computational performance and cross-validation error precision of five PLS algorithms using designed and real data sets. **Journal of Chemometrics**, n. October 2008, p. n/a-n/a, 2010.

MBOGNING, W. et al. Talanta Excitation-emission matrix fluorescence coupled to chemometrics for the exploration of essential oils. **Talanta**, v. 130, p. 148–154, 2014.

MELO, S. A. S. et al. Degradação de fármacos residuais por processos oxidativos avançados. **Química Nova**, v. 32, n. 1, p. 188–197, 2009.

MONTAGNER, C. C. et al. Contaminantes emergentes em matrizes aquáticas do Brasil: cenário atual e aspectos analíticos, ecotoxicológicos e regulatórios. **Química Nova**, v. 40, n. 9, p. 1094–1110, 11 jul. 2017.

MURATI, M. et al. Degradation and mineralization of sulcotrione and mesotrione in aqueous medium by the electro-Fenton process: A kinetic study. **Environmental Science and Pollution Research**, v. 19, n. 5, p. 1563–1573, 2012.

MURPHY, K. R. et al. Fluorescence spectroscopy and multi-way techniques. PARAFAC. **Analytical Methods**, v. 5, n. 23, p. 6557, 2013.

OLIVIERI, A. C.; ESCANDAR, G. M. Application Example. In: **Practical Three-Way Calibration**. [s.l.] Elsevier, 2014a. p. 251–271.

OLIVIERI, A. C.; ESCANDAR, G. M. Parallel Factor Analysis. In: **Practical Three-Way Calibration**. [s.l.] Elsevier, 2014b. p. 65–92.

PANIZZA, M.; CERISOLA, G. Electro-Fenton degradation of synthetic dyes. **Water Research**, v. 43, p. 339–344, 2008.

PANIZZA, M.; CERISOLA, G. Direct And Mediated Anodic Oxidation of Organic Pollutants. **Chemical Reviews**, v. 109, n. 12, p. 6541–6569, 9 dez. 2009.

PERALTA-HERNÁNDEZ, J. M.; GODÍNEZ, L. A. Electrochemical Hydrogen Peroxide Production in Acidic Medium Using a Tubular Photo-reactor: Application in Advanced Oxidation Processes. **Chem. Soc. J. Mex. Chem. Soc**, v. 58, n. 583, p. 348–355, 2014.

PUPO NOGUEIRA, R. F. et al. Fundamentos e aplicações ambientais dos processos Fenton e foto-Fenton. **Química Nova**, v. 30, n. 2, p. 400–408, 2007.

RENOVATO, R. D. O uso de medicamentos no Brasil: uma revisão crítica. **Revista**

Brasileira de Ciências Farmacêuticas, v. 89, n. 1, p. 64–69, 2008.

RICHARDSON, S. D.; TERNES, T. A. Water Analysis: Emerging Contaminants and Current Issues. **Analytical Chemistry**, v. 81, n. 12, p. acs.analchem.7b04577, 2017.

RIVERA-UTRILLA, J. et al. Pharmaceuticals as emerging contaminants and their removal from water. A review. **Chemosphere**, v. 93, n. 7, p. 1268–1287, 2013.

ROBERTS, P.; THOMAS, K. The occurrence of selected pharmaceuticals in wastewater effluent and surface waters of the lower Tyne catchment. **Science of The Total Environment**, v. 356, n. 1–3, p. 143–153, 1 mar. 2006.

ROQUE, J. V.; DIAS, L. A. S.; TEÓFILO, R. F. Multivariate Calibration to Determine Phorbol Esters in Seeds of *Jatropha curcas* L. Using Near Infrared and Ultraviolet Spectroscopies. **Journal of the Brazilian Chemical Society**, v. 28, n. 08, p. 1506–1516, 2017.

SAHU, P. K. et al. An overview of experimental designs in HPLC method development and validation. **Journal of Pharmaceutical and Biomedical Analysis**, v. 147, p. 590–611, jan. 2018.

SALAZAR, C. et al. Electrochemical degradation of the antihypertensive losartan in aqueous medium by electro-oxidation with boron-doped diamond electrode. **Journal of Hazardous Materials**, v. 319, p. 84–92, 2016.

SAUVÉ, S.; DESROSIERS, M. A review of what is an emerging contaminant. **Chemistry Central Journal**, v. 8, n. 1, p. 15, 2014.

SENA, M. M.; TREVISAN, M. G. PARAFAC: UMA FERRAMENTA QUIMIOMÉTRICA PARA TRATAMENTO DE DADOS MULTIDIMENSIONAIS. APLICAÇÕES NA DETERMINAÇÃO DIRETA DE FÁRMACOS EM PLASMA HUMANO POR ESPECTROFLUORIMETRIA Marcelo M. Sena. **Química Nova**, v. 28, n. 5, p. 910–920, 2005.

SIRÉS, I. et al. Electrochemical advanced oxidation processes: Today and tomorrow. A review. **Environmental Science and Pollution Research**, v. 21, n. 14, p. 8336–8367, 2014.

SKOOG, D. A. et al. **Fundamentals of analytical chemistry**. 9ed, Thomson, 2011.

SKOUMAL, M. et al. Electro-Fenton, UVA photoelectro-Fenton and solar photoelectro-Fenton degradation of the drug ibuprofen in acid aqueous medium using platinum and boron-doped diamond anodes. **Electrochimica Acta**, v. 54, p. 2077–2085, 2009.

SODRÉ, F. F.; LOCATELLI, M. A. F.; JARDIM, W. F. Occurrence of Emerging

Contaminants in Brazilian Drinking Waters: A Sewage-To-Tap Issue. **Water, Air, and Soil Pollution**, v. 206, n. 1–4, p. 57–67, 2 fev. 2010.

SOPAJ, F. et al. Effect of the anode materials on the efficiency of the electro-Fenton process for the mineralization of the antibiotic sulfamethazine. **Applied Catalysis B: Environmental**, v. 199, p. 331–341, 2016.

SOUZA, T. S. et al. MCR-ALS APPLIED TO THE QUANTITATIVE MONITORING OF THE ELECTRODEGRADATION PROCESS OF ATRAZINE USING UV SPECTRA: COMPARATIVE RESULTS WITH HPLC-DAD AS A REFERENCE METHOD. **Química Nova**, v. 39, n. 2, p. 137–145, 2016.

STEDMON, C. A.; MARKAGER, S.; BRO, R. Tracing dissolved organic matter in aquatic environments using a new approach to fluorescence spectroscopy. v. 82, p. 239–254, 2003.

TARLEY, C. R. T. et al. Chemometric tools in electroanalytical chemistry: Methods for optimization based on factorial design and response surface methodology. **Microchemical Journal**, v. 92, n. 1, p. 58–67, 2009.

TEN BERGE, J. M. F. Partial uniqueness in CANDECOMP/PARAFAC. **Journal of Chemometrics**, v. 18, n. 1, p. 12–16, 2004.

TEÓFILO, R. F.; FERREIRA, M. M. C. QUIMIOMETRIA II: PLANILHAS ELETRÔNICAS PARA CÁLCULOS DE PLANEJAMENTOS EXPERIMENTAIS, UM TUTORIAL. **Quim. Nova**, v. 29, n. 2, p. 338–350, 2006.

TREVISAN, M. G. “ **Aplicação de Métodos Quimiométricos de Ordem Superior e Fluorescência Molecular na Análise em Matrizes Biológicas** ”. Campinas, SP. Dissertação (Mestrado em Química) - Universidade Estadual de Campinas, SP..

VIEIRA, P. C.; CASS, Q. B.; DEGANI, A. L. G. Cromatografia: um breve ensaio. **Química Nova na Escola**, v. 7, p. 21–25, 1998.

WINDIG, W.; STEPHENSON, D. A. Self-modeling mixture analysis of second-derivative near-infrared spectral data using the SIMPLISMA approach. **Analytical Chemistry**, v. 64, n. 22, p. 2735–2742, 15 nov. 1992.

ZANIN, H. et al. Diamond cylindrical anodes for electrochemical treatment of persistent compounds in aqueous solution. **Journal of Applied Electrochemistry**, v. 43, n. 3, p. 323–330, 21 mar. 2013.

ZHAO, X. et al. Photoelectrochemical degradation of anti-inflammatory pharmaceuticals at Bi₂MoO₆-boron-doped diamond hybrid electrode under visible light irradiation. **Applied Catalysis B: Environmental**, v. 91, n. 1–2, p. 539–545, set. 2009.